

FEASIBILITY OF AN ELECTROMAGNETIC DIAPHRAGM COMPRESSOR FOR CRYOCOOLERS

Dantam K. Rao

Precision Magnetic Bearing Systems Inc.
36 Green Mountain Dr.
Cohoes, NY 12047

May 1995

Final Report



Distribution authorized to DoD components only; Proprietary Information; May 1995. Other requests for this document shall be referred to AFMC/STL.

WARNING - This document contains technical data whose export is restricted by the Arms Export Control Act (Title 22, U.S.C., Sec 2751 et seq.) or The Export Administration Act of 1979, as amended (Title 50, U.S.C., App. 2401, et seq.). Violations of these export laws are subject to severe criminal penalties. Disseminate IAW the provisions of DoD Directive 5230.25 and AFI 61-204.

DESTRUCTION NOTICE - For classified documents, follow the procedures in DoD 5200.22-M, Industrial Security Manual, Section II-19 or DoD 5200.1-R, Information Security Program Regulation, Chapter IX. For unclassified, limited documents, destroy by any method that will prevent disclosure of contents or reconstruction of the document.

19951114 085



PHILLIPS LABORATORY
Space and Missiles Technology Directorate
AIR FORCE MATERIEL COMMAND
KIRTLAND AIR FORCE BASE, NM 87117-5776

UNCLASSIFIED



AD NUMBER

AD-B205 142

NEW LIMITATION CHANGE

TO

DISTRIBUTION STATEMENT A -
Approved for public release; Distri-
bution unlimited.

Limitation Code: 1

FROM

DISTRIBUTION STATEMENT -

Limitation Code:

AUTHORITY

Janet E. Mosher, Phillips Lab., Kirtland AFB, N. M.

THIS PAGE IS UNCLASSIFIED

PL-TR-95-1058

This final report was prepared by Precision Magnetic Bearing Systems Inc, Cohoes, NY, under Contract F29601-94-C-0138 Job Order, 21021002, with Phillips Laboratory, Kirtland Air Force Base, New Mexico. The Laboratory Project Officer-in-Charge was Brian Whitney (VTPT).

When Government drawings, specifications, or other data are used for any purpose other than in connection with a definitely Government-related procurement, the United States Government incurs no responsibility or any obligation whatsoever. The fact that the Government may have formulated or in any way supplied the said drawings, specifications, or other data, is not to be regarded by implication, or otherwise in any manner construed, as licensing the holder, or any other person or corporation; or as conveying any rights or permission to manufacture, use, or sell any patented invention that may in any way be related thereto.


This report has been authored by a contractor of the United States Government. Accordingly, the United States Government retains a nonexclusive royalty-free license to publish or reproduce the material contained herein, or allow others to do so, for the United States Government purposes.


This report contains proprietary information and shall not be either released outside the government, or used, duplicated or disclosed in whole or in part for manufacture or procurement, without the written permission of the contractor. This legend shall be marked on any reproduction hereof in whole or in part.


If your address has changed, if you wish to be removed from the mailing list, or if your organization no longer employs the addressee, please notify PL/VTPT, 3550 Aberdeen Ave SE, Kirtland AFB, NM 87117-5776 to help maintain a current mailing list.

This report has been reviewed and is approved for publication.

FOR THE COMMANDER


BRIAN WHITNEY
Project Officer


DAVID KRISTENSEN, Lt Col, USAF
Chief, Space Power and Thermal
Management Division


HENRY L. PUGH, JR., Col, USAF
Director of Space and Missiles Technology

DO NOT RETURN COPIES OF THIS REPORT UNLESS CONTRACTUAL
OBLIGATIONS OR NOTICE ON A SPECIFIC DOCUMENT REQUIRES THAT IT BE
RETURNED.

The following notice applies to any unclassified (including originally classified and now declassified) technical reports released to "qualified U.S. contractors" under the provisions of DoD Directive 5230.25, Withholding of Unclassified Technical Data From Public Disclosure.

NOTICE TO ACCOMPANY THE DISSEMINATION OF EXPORT-CONTROLLED TECHNICAL DATA

1. Export of information contained herein, which includes, in some circumstances, release to foreign nationals within the United States, without first obtaining approval or license from the Department of State for items controlled by the International Traffic in Arms Regulations (ITAR), or the Department of Commerce for items controlled by the Export Administration Regulations (EAR), may constitute a violation of law.
2. Under 22 U.S.C. 2778 the penalty for unlawful export of items or information controlled under the ITAR is up to two years imprisonment, or a fine of \$100,000, or both. Under 50 U.S.C., Appendix 2410, the penalty for unlawful export of items or information controlled under the EAR is a fine of up to \$1,000,000, or five times the value of the exports, whichever is greater; or for an individual, imprisonment of up to 10 years, or a fine of up to \$250,000, or both.
3. In accordance with your certification that establishes you as a "qualified U.S. Contractor", unauthorized dissemination of this information is prohibited and may result in disqualification as a qualified U.S. contractor, and may be considered in determining your eligibility for future contracts with the Department of Defense.
4. The U.S. Government assumes no liability for direct patent infringement, or contributory patent infringement or misuse of technical data.
5. The U.S. Government does not warrant the adequacy, accuracy, currency, or completeness of the technical data.
6. The U.S. Government assumes no liability for loss, damage, or injury resulting from manufacture or use for any purpose of any product, article, system, or material involving reliance upon any or all technical data furnished in response to the request for technical data.
7. If the technical data furnished by the Government will be used for commercial manufacturing or other profit potential, a license for such use may be necessary. Any payments made in support of the request for data do not include or involve any license rights.
8. A copy of this notice shall be provided with any partial or complete reproduction of these data that are provided to qualified U.S. contractors.

D E S T R U C T I O N N O T I C E

For classified documents, follow the procedures in DoD 5200.22-M, Industrial Security Manual, Section II-19 or DoD 5200.1-R, Information Security Program Regulation, Chapter IX. For unclassified, limited documents, destroy by any method that will prevent disclosure of contents or reconstruction of the document.

DRAFT SF 298

1. Report Date (dd-mm-yy) May 1995		2. Report Type Final		3. Dates covered (from... to) 6/94 to 12/95	
4. Title & subtitle Feasibility of an Electromagnetic Diaphragm Compressor for Cryocoolers				5a. Contract or Grant # F29601-94-C-0138	
				5b. Program Element # 62601F	
6. Author(s) Dantam K. Rao				5c. Project # 2102	
				5d. Task # 10	
				5e. Work Unit # 02	
7. Performing Organization Name & Address Precision Magnetic Bearing Systems Inc. 36 Green Mountain Dr Cohoes, NY 12047				8. Performing Organization Report # PREMAG-95-02	
9. Sponsoring/Monitoring Agency Name & Address Phillips Laboratory 3550 Aberdeen Ave SE Kirtland AFB, NM 87117-5776				10. Monitor Acronym	
				11. Monitor Report # PL-TR-95-1058	
12. Distribution/Availability Statement Distribution authorized to DoD components only; Proprietary Information; May 1995. Other requests shall be referred to AFMC/STI.					
13. Supplementary Notes					
14. Abstract This Phase I SBIR report documents the establishment of feasibility of a electromagnetic diaphragm compressor which is designed to drive cryocoolers. Two prototype compressors were built and tested as part of this feasibility establishment program. The first prototype used permanent magnet bias while the second prototype used electromagnet bias. Testing the first prototype indicated that the diaphragm used in it is too stiff for satisfactory operation. As a result, electromagnet was used as biasing device in the second prototype and the stiff diaphragm is replaced by a more flexible one. In addition to this prototype building activity, a computer code to analyze and size this type of compressor has been developed in this phase I effort. Testing the prototype has indicated that it can develop pressure ratios of up to 1.7 at frequencies of up to 60 diaphragms Hz. Since the prototype demonstrated performance parameters that are within the realm of cryocoolers, we conclude that it is feasible to engineer an electromagnetic diaphragm compressor that can meet the design requirements of cryocoolers. As a result, it is recommended to move the project to Phase II.					
15. Subject Terms Compressors, pumps, cryocoolers, diaphragms, electromagnets, magnetic bearings.					
Security Classification of			19. Limitation of Abstract	20. # of Pages	21. Responsible Person (Name and Telephone #)
16. Report Unclassified	17. Abstract Unclassified	18. This Page Unclassified	Limited	62	Brian Whitney (505) 846-1867

GOVERNMENT PURPOSE LICENSE RIGHTS
(SBIR PROGRAM)

Contract Number: F29601-94-C-0138

Contractor: Precision Magnetic Bearing Systems Inc.
Cohoes, NY

For a period of four (4) years after delivery and acceptance of the last deliverable item under the above contract, this technical data shall be subject to the restrictions contained in the definition of "Limited Rights" in DFARS clause at 252.227-7013. After the four-year period, the data shall be subject to the restrictions contained in the definition of "Government Purpose License Rights" in DFARS clause at 252.227-7013. The Government assumes no liability for unauthorized use or disclosure by others. This legend shall be included on any reproduction thereof and shall be honored only as long as the data continues to meet the definition on Government purpose license rights.

ACKNOWLEDGMENTS

This report has been made possible due to an SBIR Phase I program sponsored by Ballistic Missiles Defense Organization, Carl Nelson, Program Manager. Carl Nelson's strong interest in nascent technologies and rapid commercialization has been instrumental in the successful development of this technology. The authors also acknowledge significant contributions by Brian Whitney and Captain Pete Thomas in the Phillips Laboratory. Extensive technical discussions with them had clarified the specifications of the compressor for cryocoolers that is developed under this project.

Special acknowledgement is also due to many of the PREMAG's personnel whose contributions made it possible to successfully conclude this project. Curt Richardson, design engineer had been of great help in evolving the design of the compressor described herein. The fabrication and testing phases of the compressors has been carried out with considerable precision by Dave Slezak and Leo Hoogenboom. The review of the report has been conducted with characteristic thoroughness by Dr. B. Banerjee.

The rapid commercialization of the technology developed herein has been made possible with the support of many of our colleagues in the commercial and financial community. The author especially acknowledge the negotiation skills of Dr. Richard Callahan and Peter McDavitt of CTC that have been the key in the licensing negotiations. Sound business advice from Richard Derrick, CPA, Richard Saburro of Capital Region Technology Development Council, Dr. Suresh Bhate of Electromagnetic Technologies, Jay Murphy of Macrodyne have also been of great help in developing the commercialization strategy. Fast and timely support from their licensing and patent attorneys has also been a significant factor in the rapid commercialization of the technology.

Accession For	
NTIS CRA&I	<input type="checkbox"/>
DTIC TAB	<input checked="" type="checkbox"/>
Unannounced	<input type="checkbox"/>
Justification _____	
By _____	
Distribution /	
Availability Codes	
Dist	Avail and/or Special
E-4	

CONTENTS

1. OVERVIEW	1
1.1 Introduction	1
1.2 Existing Compressor Approaches	1
1.3 Diaphragm Compressor Design	2
1.4 Advantages of Diaphragm Compressors	2
1.5 Phase I Technical Objectives	3
1.6 Phase I Technical Approach	3
1.7 Phase I Results	4
2. DIAPHRAGM COMPRESSOR CONCEPT	11
2.1 Compressor Overview	11
2.2 Critical Components	12
3. COMPRESSOR DESIGN REQUIREMENTS	16
3.1 Design Requirements	16
3.2 Output PV Power	19
3.3 Efficiency	21
3.4 Pressure Wave	21
4. DIAPHRAGM	23
4.1 Design Requirements	23
4.2 Load Analysis	24
4.2.1 DC Load	25
4.2.2 AC Load	25
4.3 Deflection Analysis	32
4.4 Stress Analysis	34
4.5 Diaphragm material	36
4.6 Dynamic Model of the Diaphragm	42
5. COMPRESSION CHAMBER	45
5.1 Design Requirements	45
5.2 Back chamber	47
CONCLUSIONS	50
REFERENCES	51

CONTENTS

FIGURES

Figure 1	Compressor Design Software	5
Figure 2	Permanent Magnet Compressor Prototype	7
Figure 3	All Electromagnet Compressor Prototype	8
Figure 4	Schematic: Electromagnetic Diaphragm Compressor	12
Figure 5	Electromagnetic Diaphragm Compressor Configuration	13
Figure 6	Key Component Block Diagram	14
Figure 7	Typical Pressure Wave Form	18
Figure 8	PV Diagrams of Stirling Cycle Cryocoolers	20
Figure 9	Method of Generation of Attraction Forces	27
Figure 10	Gas Spring Force	30
Figure 11	Normalized Net Gas Force vs Displacement	32
Figure 12	Fatigue Curves	40
Figure 13	Free Body Diagram of the Diaphragm	43
Figure 14	Back chamber Designs	49

1. OVERVIEW

1.1 Introduction

This Phase I Technical Report documents the successful establishment of the feasibility of a novel diaphragm compressor configuration for cryocoolers. We established the feasibility by successfully building a Proof of Principle (PoP) model of this novel compressor. This report presents the analytical basis and the results of an experimental test program conducted to confirm the potential benefits of the diaphragm compressor design. We conclude that novel compressors of essentially infinite life can be produced by this innovative design concept.

1.2 Existing Compressor Approaches

A typical cryocooler consists of a compressor, displacer and pressurized gaseous helium (GHe). The compressor generates a pressure wave in GHe which is used to reciprocate the displacer to produce cold. Its function is to efficiently generate the pressure wave.

Space quality cryocoolers should have extremely long life and high reliability to achieve the space mission objectives. Ideally long life requires elimination of all rubbing parts that produce friction and wear. Existing Stirling cryocoolers avoid rubbing by using flexures to suspend the reciprocating piston. These pistons use a very small clearance to reduce gas leakage. Such clearance seals however are sensitive to manufacturing inaccuracies. Elimination of pistons, flexures and clearance seals will obviously result in a compressor that is free of wear-prone parts. The objective of our diaphragm compressor concept is to develop such a design methodology.

1.3 Diaphragm Compressor Design

In our approach, a diaphragm is vibrated by magnetic fields to produce the pressure wave. A diaphragm is defined as a thin circular plate (with no central hole and fixed at the edges) whose deflection is of the order of its thickness. The magnetic fields are produced by an attraction electromagnet. Unlike the existing Oxford design, the diaphragm compressor does not use pistons, clearance seals, flexures or other reciprocating members. The diaphragm sweeps and seals the working volume of the cryocooler. Because this design eliminates many of the precision parts that are commonly used in existing cryocoolers, it provides an added benefit of reduced cost and improved performance.

Building the PoP compressor model has given us valuable insight which makes us believe that our diaphragm compressor will be more reliable. Use of a diaphragm, however, carries the recognized risk of high cycle fatigue failure. In a five year cryocooler, the diaphragm accumulates about 10^{10} cycles of reversing stresses. A diaphragm that can sustain such a large number of cycles without failure would require that these stresses be low in magnitude. Our aim is to accomplish this by using large diameter and small stroke geometries.

This report documents in detail the results of analytical and experimental programs executed to develop the diaphragm compressor. The report concludes positively that it is feasible to design this novel diaphragm compressor and recommends moving forward to Phase II for developing a fully functional engineering prototype compressor.

1.4 Advantages of Diaphragm Compressors

The design concept we propose can be applied to cryocoolers of the following types: Stirling cycle, pulse-tube, acoustic or magnetic. (It can also be applied to several other applications such as small industrial pumps, refrigerator compressors, automotive pumps etc.). Its primary function is to generate a pressure wave in a charged fluid using large bore and short-stroke diaphragm geometries .

This diaphragm compressor does not use the classical piston-in-cylinder approach. Hence it does not employ any reciprocating parts such as pistons or linear motors. Thus it does not have

any rubbing parts. The elimination of rubbing parts increases the life of the compressor. Diaphragm compressors also offer higher power densities because the attraction electromagnets generate larger force in a given volume than conventional linear motors [1]. Higher power densities translate to smaller weight and a lighter compressor.

Diaphragm compressors need fewer precision parts than the piston compressors. Precise alignment of a piston and a cylinder is not necessary for these compressors. Hence they will be more rugged and less expensive.

1.5 Phase I Technical Objectives

The primary objective of the Phase I effort is to establish the feasibility of this diaphragm compressor. This effort therefore answers the critical feasibility questions, namely, will this compressor work in the way it is supposed to work, and can the diaphragm be sized for a space-type cryocooler while maintaining low stress? The specific technical objectives of Phase I are therefore:

- o Design and fabricate a proof of principle model of the compressor
- o Determine maximum stresses, and swept volumes produced

1.6 Phase I Technical Approach

The Phase I began by a kick-off meeting with the government technical personnel wherein the performance goals were discussed. During this meeting it was agreed that the construction of a proof of principle model of the compressor is the key requirement to establish feasibility. Based on these discussions, a preliminary design of the PoP compressor was developed. The base line requirements such as frequency, charge pressures, pressure ratios and the swept volumes were established first with the help of the Project Monitor. These parameters were then employed to analytically evaluate the maximum stresses, deflections and volumes under the combined action of the attraction and gas loads. A proof of principle compressor was then fabricated and tested up to 300 Hz to establish the soundness of this approach.

The work was performed as five tasks that are designed to meet specific technical objectives. These tasks are:

1. Determine the requirements for the compressor
2. Determine the requirements for the diaphragm and size it
3. Analyze the stresses generated in the diaphragm
4. Design and fabricate a Proof of Principle compressor
5. Test the Proof of Principle compressor

The results of these five tasks, which encompass both the analytical and experimental aspects, provide a strong indication that a diaphragm compressor that can operate for five years can be developed and fabricated.

1.7 Phase I Results

(a) *Compressor Design Software*

The purpose of this software is to predict the performance of the compressor once its geometric dimensions and the operating parameters are known. This will involve translating the design requirements into a sizing algorithm. The basic approach is to develop a theoretical analysis for sizing individual components first, developing subroutines to code them and combine all these subroutines into a system flow chart. This approach breaks down the complex task of developing a large unmanageable code into a manageable number of smaller subroutines which can be easily coded and debugged.

We have developed a baseline compressor design software as part of Phase I effort. We will be extending and refining this software into a comprehensive stand-alone software module in Phase II. Figure 1 shows a typical input/output of this baseline software. The software inputs the design specifications of the compressor and outputs its sizing and performance parameters.

```

back chamber - two sided approach
28.5e6      E =      youngs modulus, psi
0.3         anu=     poissons ratio
3.90        D=      diaphragm diameter, in.
0.015       t =      diaphragm thickness, in
1.00        r0 =     central pole's radius, in
30.0        pawdc   attraction pressure in work chamber, dc comp.,psia
15.         pawac   attraction pressure in work chamber, ac comp., psi
30.         pabdc   attraction pressure in back chamber, dc comp., psia
15.         pabac   attraction pressure in back chamber, ac comp., psi
25.0        pgwdc   gas pressure in work chamber, dc comp., psia
8.30        pgwac   gas pressure in work chamber, ac comp., psi
25.0        pgbdc   gas pressure in back chamber, dc comp., psia
8.3         pgbac   gas pressure in back chamber, ac comp., psi
0.5         alpha   defl.volume/swept vol. ratio
0.10        vp      vol. of payload,in3
1.4         gamma   specific heat ratio

```

OUTPUT

DIAPHRAGM

```

Static stress, psi      sdc=      .00
Dyn. stress amplitude, psi  sac= -15364.24
attraction load, dc, lb  Fadc=      .00
attraction load, ac, lb  Faac=     94.26
attraction deflection,ac,in  yac=     -.51
Diaphragm stiffness,lb/in  k =    185.67
gas load, dc, lb         Fgdc=      .00
gas load, ac, lb         Fgac=    198.32

```

DEFLECTION OF DIAPHRAGM (-ve = into work-chamber)

```

radius, in      deflection, in
.0010           -.0819
.1950           -.0785
.3900           -.0690
.5850           -.0544
.7800           -.0369
.9750           -.0193
1.1700          -.0053
1.3650           .0025
1.5600           .0042
1.7550           .0019
1.9500           .0000

```

WORK CHAMBER

```

Charge pressure, psi      pm =     25.00
Pressure wave amplitude,psi  po =     8.30
Max. gas pressure, psia   pmax=    33.30
Min. gas pressure, psia   pmin=    16.70
Pressure ratio            r =     1.99
mean captive volume, in3   Vm =     .7666
work chamber volume, in3   Vw =     .6666
dead volume, in3          Vd =     .5246
deflection volume, in3     VD =     .1419
swept volume, in3         delv =    .2839
WORK CHAMBER IS CONTOURED

```

Figure 1. Output of the compressor design software developed under Phase I

(b) Fabrication of Prototype Compressors

In order to establish the Feasibility of the diaphragm compressor, we built two prototype units. The first unit - shown in Figure 2 - used Permanent Magnet bias to attract a titanium alloy disk to which a soft-steel disk (made of iron powder embedded in a silicone matrix) is attached. This approach showed significant promise, but the diaphragm used was too stiff. To overcome this hurdle we revised our approach to an all-electromagnet approach in the second prototype. In this prototype - shown in Figure 3 - we used bias currents in the electromagnets to carefully control the position of the diaphragm. This approach proved to be successful and has been documented in this report.

Permanent Magnet Biased Prototype Compressor

This Prototype used two NdBF_e permanent magnet ring, 3 in. OD x 1.75 in. ID x 0.15 in. thick embedded in the steel core of two electromagnets as shown in Figure 2. The diaphragm is made of 3.66 in. diameter Titanium alloy disk which is 0.05 in. thick to which a flexible steel disk, which is 3.60 in. diameter and 0.2 in. thick is attached as shown in Figure 2. The electromagnet coil is mounted in an annular slot with 4.66 in. diameter as shown. The diaphragm is held in position by precisely machined annular rings made of non-magnetic stain less steel. The two electromagnets are bolted together by a set of 6 bolts.

Figure 2 also shows the flexible-steel disk that is fabricated during this prototype building activity. Realizing that the thickness of the disk must be large enough to allow closure of flux path, we developed this soft-steel disk as part of this Phase I activity. This flexible disk is made by mixing fine iron-powder into a silicone mould and using an appropriate catalyst to embed the iron-powder particles in the silicone matrix. The silicone matrix offered the flexibility that is needed by the diaphragm while the iron powder provided the medium for the flux path. This approach resulted in a new material aptly called flexi-steel disk since it combined the magnetic properties of rigid steel and flexibility of silicone.

During the testing of this prototype however, we found that the Titanium alloy diaphragm is too thick and hence the electromagnet is not strong enough to vibrate the diaphragm. As a result, for the purpose of Phase I activity we elected to make another prototype which used bias currents to position the diaphragm.

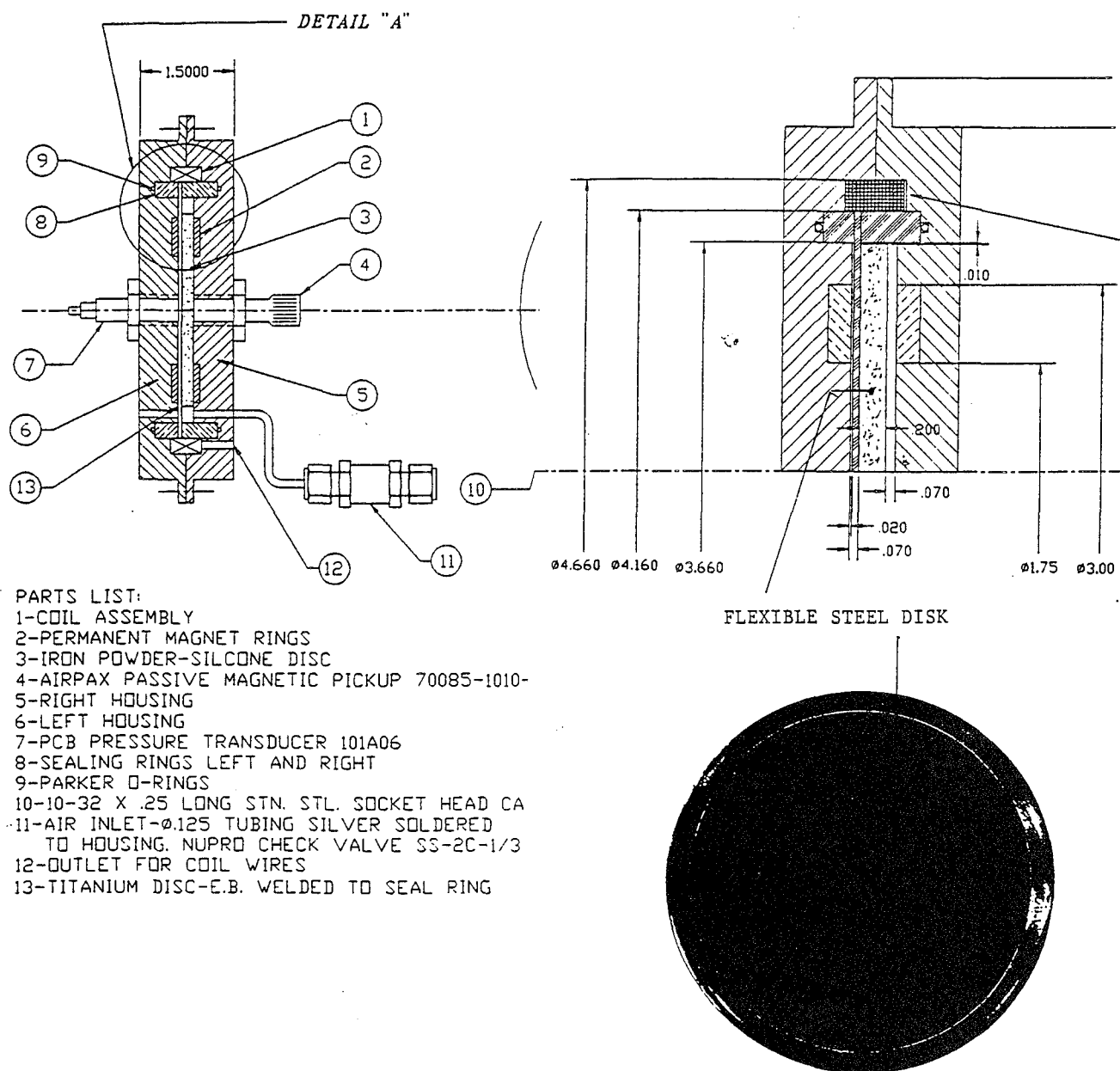


Figure 2. Permanent Magnet Bias Compressor prototype. This is the first prototype that was built, but the diaphragm that was used proved to be too stiff

All-electromagnet biased compressor prototype

The second prototype that we built used a single electromagnet to position the diaphragm and vibrate it, thus creating the pressure wave needed. This prototype is described in more detail in Section 2 and in the later parts of this report. Essentially this prototype used two electromagnets sandwiching a diaphragm and vibrating it. We attached two steel disks to the diaphragm in order to close the flux circuit and also to generate larger forces. This approach proved to be successful. This Phase I report documents the design methodology used to design, fabricate and test this type of compressor.

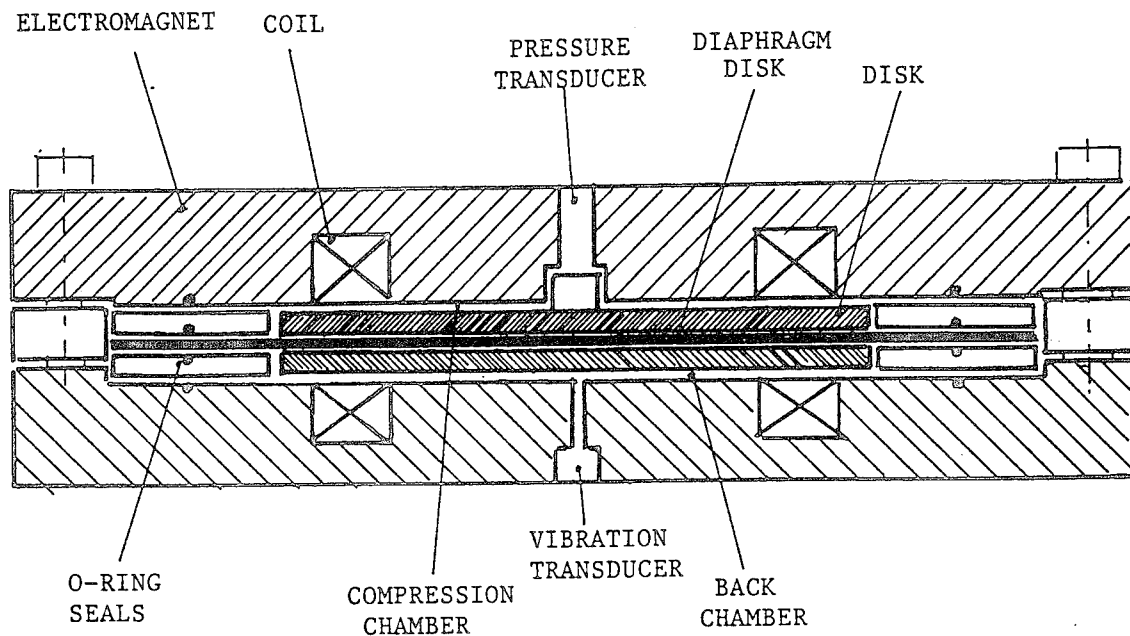


Figure 3. All Electromagnet Compressor Prototype. This is the second prototype compressor that was built under this Phase I effort. This prototype has been successfully used to generate the desired pressure wave

The unique features of this second prototype are the use of:

- a three point seal support of the diaphragm to increase its life
- a switching amplifier to reduce power loss
- a low inertia moving member to reduce force required

As shown in Figure 3, this prototype compressor used a single diaphragm, made of spring steel, 5 in. diameter and 0.020 in. thick which is supported on O- rings at 4 in. diameter. The diaphragm used a disk of 3.2 in. OD and 0.125 in. The disk enhances the attraction force produced on the diaphragm. The disk is mounted on a 10-32 screw and spaced by a plastic shim which is 0.015 thick in diameter. The thread of this screw is scratched in order to equalize the pressures in the compression and back chamber. Initially we tried a three point support for the diaphragm and found that it caused bending, thus centering it was difficult. We then replaced it by the two point seal support, with the seals spaced on either side of the diaphragm at the same diameter. Our tests indicated that ensuring symmetric gaps is the key to the successful implementation of the prototype. The electromagnets used coils in a slot which has 2 in. ID x 2.8 in. OD and 0.38 in. height. The coils are made of gage 22 magnet wire with 120 turns. The cylindrical face is contoured to take up the shape of the deflected diaphragm. The electromagnet is driven by an external switching amplifier using a laboratory signal source. A photonic vibration sensor and a pressure transducer are used to monitor the vibrations of the diaphragm and the pressure wave produced by it respectively.

While developing the prototype we investigated two options of electromagnet configurations and three options of its drive circuit. The electromagnets can be arranged in NSSN configuration so that they repel each other (the flux from one electromagnet loops back to itself) or in the NSNS configuration so that they attract each other (the flux from one electromagnet goes through other electromagnet before returning). We found that these configurations options made no difference in pressure output. We also tried three different options of driving the electromagnets - first with no capacitor, second with a capacitor on one electromagnet and a third with capacitor on both electromagnets. We found that the placement of the capacitor did make difference in the pressure output. The option in which the capacitor is connected across one electromagnet yielded the greatest pressure output while the other two options yielded poor results. Hence we chose this drive circuit option.

After gaining a thorough understanding of the operating principle of this prototype, we started investigating the maximum pressure output that the prototype can deliver. Our initial tests however indicated that the maximum pressure output strongly depends on the dead space in the compression chamber. During this prototype building activity we did not have full control on the dead space, and hence the performance is lower than what can be expected. Even with this deficiency, we have successfully vibrated the diaphragm at up to 300 Hz and developed pressure

amplitudes of up to 3 psi at atmospheric pressure. We then filled the compressor with air pressurized at 20 psi; in this charged mode, we could vibrate the diaphragm at frequencies of up to 60 Hz and generate pressure waves of up to 5 psi in amplitude. Thus we showed that even this preliminary prototype can yield pressure ratios of up to 1.7.

In summary, we achieved pressure ratios of up to 1.7 at frequencies of up to 60 Hz. Since the space quality cryocoolers require pressure ratios of 2 and frequencies of 40 Hz, the demonstrated parameters are within the realm of the cryocoolers. Hence we believe that this technology has high potential and can be refined in Phase II and integrated into the cryocooler.

2. DIAPHRAGM COMPRESSOR CONCEPT

2.1 Compressor Overview

Figure 4 shows a schematic of this compressor. The compressor's primary function is to generate a pressure wave. It uses large bore and short-stroke diaphragm geometries. It comprises of the mechanical compressor itself and its electronic controller. The mechanical compressor is connected to the payload volume of a cryocooler. The compressor hardware is driven by the electronic controller. The electronic controller is a separate unit that is attached by cables to the mechanical compressor. It houses the signal generator and power amplifiers which produce the oscillatory current needed for the compressor.

The compressor operates as follows. Two attraction electromagnets vibrate the diaphragm in pull-pull mode, thus generating the required pressure wave. This pressure wave is transmitted through the charged fluid into the displacer volume of the cryocooler.

Figure 5 shows the mechanical compressor; it comprises of a vibrating diaphragm, compression chamber and the cylinder. The diaphragm is firmly attached to the cylinder head at the outer periphery. The cylinder head is contoured and contains electromagnets (comprising a coil and a core). The diaphragm is separated from the cylinder head by a small compression volume. A small gap between the diaphragm and the electromagnet thus constitutes a compression chamber in which the diaphragm vibrates. This volume contains the pressurized gas that is alternately compressed and expanded by the diaphragm. These compressions and expansions create the desired pressure wave.

The electronic controller comprises of a signal generator and a power amplifier. It is energized by a DC power supply. If necessary, a closed loop controller can be added to accurately control the position of the diaphragm with respect to the current signal. The signal generator and power amplifier are chosen so that their frequency and power capacity are commensurate with the application requirements.

Figure 6 shows how the key components of the compressor work together. The signal generator produces a sinusoidal voltage signal at a desired frequency. The power amplifier uses this signal to produce a sinusoidal current. This current is fed into the coils of the electromagnet, thus generating ampere-turns. The soft-iron core converts the ampere-turns into flux density. The flux density in the gap produces an attraction force. This force causes the diaphragm to vibrate. These vibrations create the swept volume. The swept volume in the confined spaces of the compression chamber results in the desired pressure wave. We give below the salient features of the key components.

2.2 Critical Components

Cylinder. The cylinder comprises of a contoured head and attraction electromagnets. It provides the working volume needed for the compressor. The contoured head permits expulsion of all the fluid from the compression chamber during the compression stroke of the diaphragm. The contoured cavity is sealed by the diaphragm to prevent any leakage paths. A resin mold is applied to the coil to prevent gas seepage. The dead volume can be minimized by contouring the cavity using NC machining to achieve a large pressure-wave.

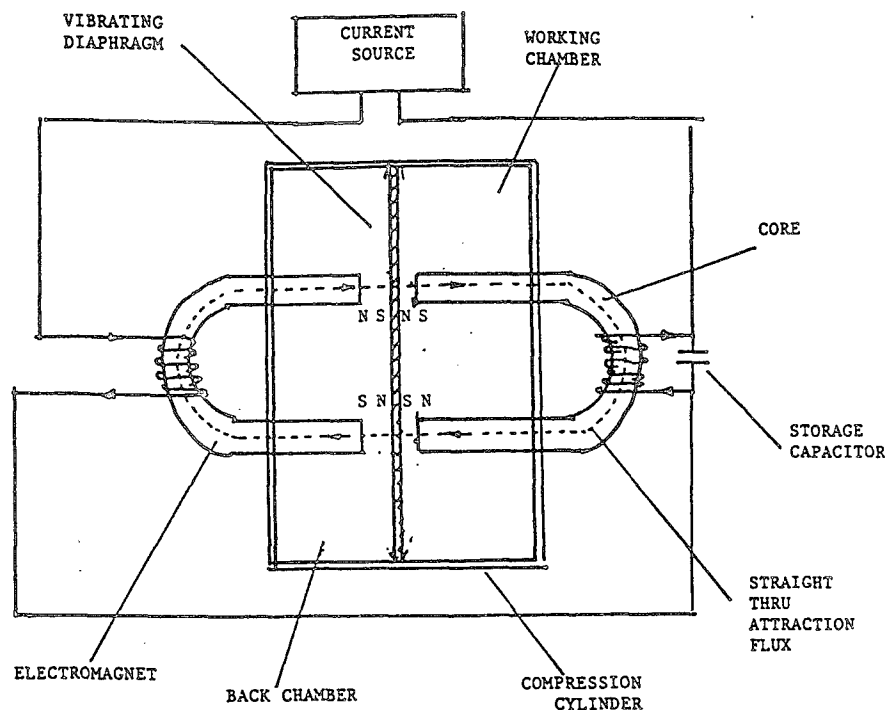


Figure 4. Schematic of the Electromagnetic Diaphragm Compressor

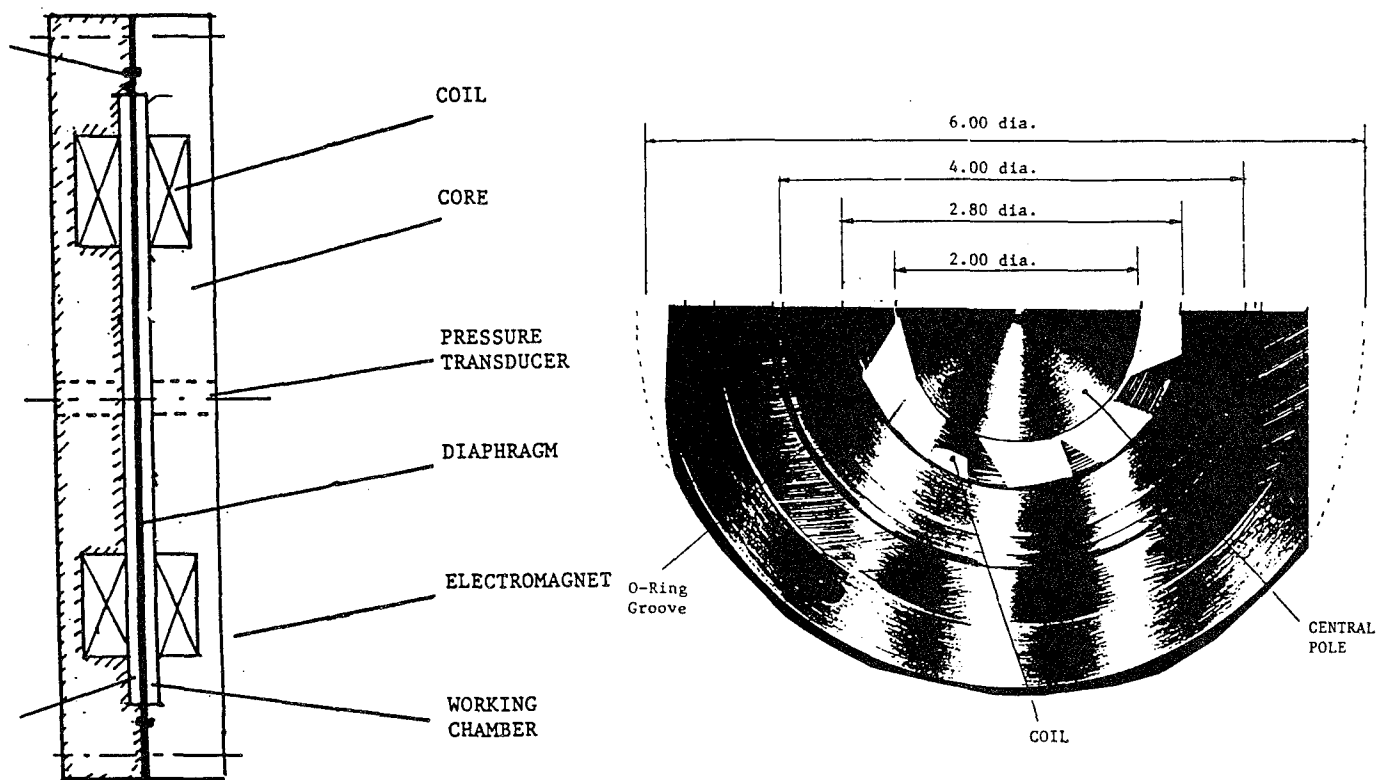


Figure 5. Electromagnetic Diaphragm Compressor Configuration

Diaphragm. The diaphragm is the critical component that sweeps the working volume to generate the pressure wave. It is made of high-fatigue strength material such as spring steel [3] since its primary function is to demonstrate that the compressor can operate with long life. The diaphragm's surface is finished smooth and is free of nicks and scratches to reduce surface stresses. The thickness variations are meticulously controlled. It is equi-spaced between the compression and back chambers. At the outer edge, the diaphragm is fixed to the cylinder head. A special fixturing design prevents fretting failure. This design uses two to four O-rings. The O-rings are pre-loaded to seal the diaphragm. They are housed in a circular groove so that as the diaphragm vibrates, no part of the diaphragm touches the housing. This special design feature prevents fretting failure.

Electromagnet. The electromagnets generate the pull-force on the diaphragm. Each electromagnet comprises of the coil and the core. The coil is of drop-in design and does not contain a bobbin to improve the ampere-turns. It is vacuum-impregnated with high temperature epoxy and is insulated from the core. It is hi-pot tested for insulation breakdown and then potted

to prevent any gas leakage. To seal it, a high quality epoxy is used. The excess epoxy is removed by machining. The magnet wire leads are protected against rough handling. The core is made of low-carbon steel and is over-sized to prevent saturation. The electromagnet has a central pole and an outer pole. Our investigations found that the outer pole is not effective in displacing the diaphragm as it is too close to the fixed edge of the diaphragm. As such its effect will be neglected in the design of the compressor.

Controller. The controller provides the drive current needed by the electromagnet coils. A BK Precision 3011B signal generator was used as the signal source in Phase I. This signal generator can be replaced by alternative commercially available signal-generating chips - this approach will be investigated in Phase II for optimal performance. This generator can supply the required sine signal at frequencies of up to 1000 Hz or more. The power amplifier is made by Advanced Motion Controls, model 30A20-AC.; it is pulse width modulated,

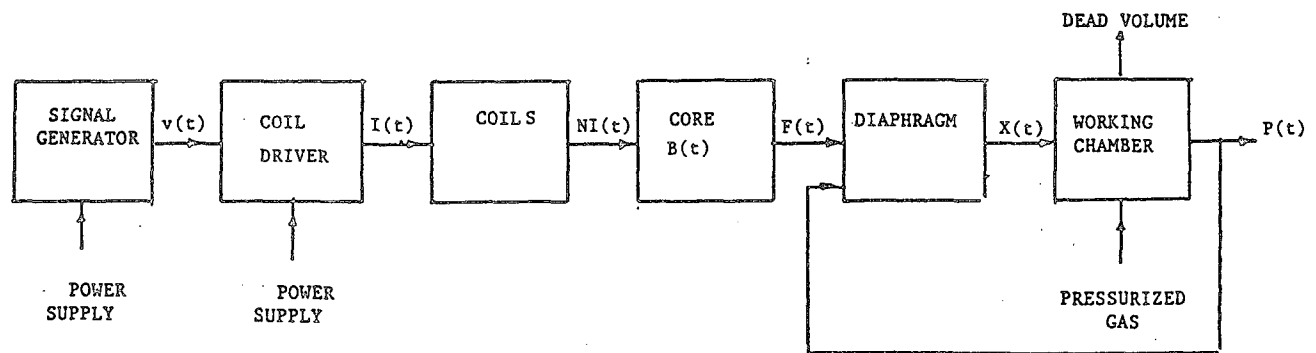


Figure 6. Block Diagram Showing Interrelation of Key Components.

with 33 kHz switching frequency. It has peak power output of 5.1 kW (+/- 170 V at 30 A), bandwidth of 2.5 kHz and gain of 8 A/V , and weighs 2.5 lb. This current amplifier outputs the current signal from a given voltage signal. In the second prototype this amplifier will be replaced

by an optimized unit for minimal power consumption. Its 5.1 kW output power capacity is ample and can easily drive the 30 watts coils. Its gain of 8 amp/volt is large enough to apply the desired sinusoidal amperes into the coil. Its frequency bandwidth of DC to 2500 Hz spans the near-DC frequencies needed for the diaphragm.

3. COMPRESSOR DESIGN REQUIREMENTS

The objective of the Phase I program is to show that the diaphragm compressor is realistic and is of value to the space cryocooler community. In our design a circular diaphragm, vibrated by an electromagnet is used to produce meaningful pressure waves while sustaining low level stresses. To provide a design basis, we first developed a design methodology which is described in this section.

In Phase I we selected a 1 W/80 K cryocooler as the target. This specification encompasses the space quality cryocoolers as well as tactical cryocoolers. The latter type are required in large numbers and current designs exhibit significant problems with reliability, life and cost. We therefore believe that we can cover the space applications as well as commercial applications by this specification. Even though the capacity chosen was relatively arbitrary, our analysis indicates that we can successfully scale it up over a range of cooling capacities.

3.1 Design Requirements

The design of the compressor begins by specifying its performance parameters. These parameters are : (1) the output PV power P_{PV} , (2) the efficiency η , defined as the ratio of the output PV power and the input electrical power P_{in} (3) the operating frequency f (4) the mean fill pressure p_m (5) the pressure ratio r , defined as the ratio of maximum pressure to the minimum pressure and (6) the phase angle ϕ by which the pressure wave leads the diaphragm's central deflection.

To generate the pressure wave, the compressor consumes electrical power and outputs mechanical PV power. The ratio of the output PV power and the electrical power is called the efficiency. Obviously, a compressor should be as efficient as possible. Existing piston-in-cylinder designs usually are 70 % efficient. Thus to output a typical 20 watts of PV power, its coils consume almost 30 watts of electrical power.

The efficiency of electromechanical power conversion depends on how well the compressor chamber is tuned with the "load" (i.e., displacer). The compressor is like a battery. The displacer is the load which draws power from this battery. The impedance of the displacer (the load) must therefore be matched with the compressor's (battery's) impedance for optimum power transfer. Knowledge of the displacer volume is therefore essential for an optimal design of compressor. However, since the thrust of this phase I effort is to establish the operating principle, we have not investigated the effect of the displacer load on the compressor design.

Recently a LOM (Linear Oscillating Motor) compressor using an annular diaphragm i.e., a diaphragm with a central hole was developed [1]. Note that, in contrast, PREMAG's design uses a diaphragm without the central hole. The elimination of the central hole avoids stress concentration and hence increases life. Further, the prior-art design used a Linear Oscillating Motor which uses a complex flux circuit; in contrast we used attraction electromagnet which use a simplified flux circuit. To drive the LOM the prior art used two signal generators and two power amplifiers; in contrast we use only one signal source and one power amplifier. A typical pressure wave produced by the prior-art compressor is shown in Figure 7. The design parameters of the PoP model, derived from this figure, are:

p_m = Mean pressure, ps i	= 25 psia
r = Pressure ratio	= 2
f = Frequency, cps	= 25 Hz
s = Stroke, mm	= 0.016 in. (0.4 mm)

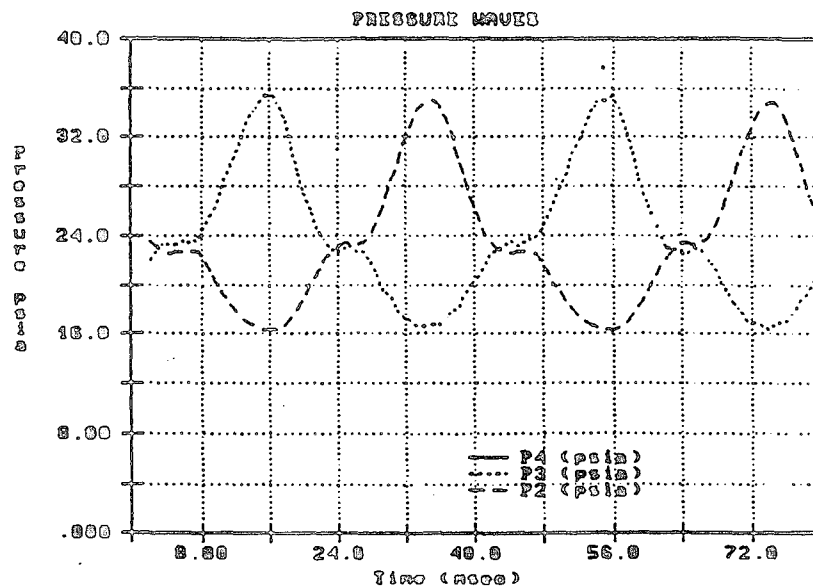


Figure 7. Typical pressure wave form from an LOM compressor

We may add that in Phase II we propose to develop a well engineered compressor that can drive a space-quality cryocooler. Typical requirements for such phase II compressor will be [for a 0.8 W/80 K cryocooler, see ref. [6]:

P_{PV}	=Output PV power, W	= 20 watts
η	= Compressor efficiency	= 70 %
p_m	=Mean fill pressure, psi	= 150 psi (1 MPa)
r	= Pressure ratio	= 2
f	= Frequency, cps	= 40 Hz
ΔV	=Swept volume, mm ³	= 0.12 in ³ (2 cc)
ϕ	= pressure wave lag	= TBD

In addition to the above, an optimally designed compressor requires that:

- (a) The diaphragm must have infinite fatigue life (i.e., maximum stress < 10,000 psi).
- (b) The compressor must consume minimal power (i.e., $\eta > 70\%$).
- (c) The compressor must be light-weight (i.e., < 6.6 lb).
- (d) The vibrations of the compressor must be minimal (< 2 N or 0.05 lb).

In the next few sections we discuss the implications of these specifications.

3.2 Output PV Power

The output PV power equals product of the area of the PV diagram and the frequency f :

$$P_{PV} = f \int p dV$$

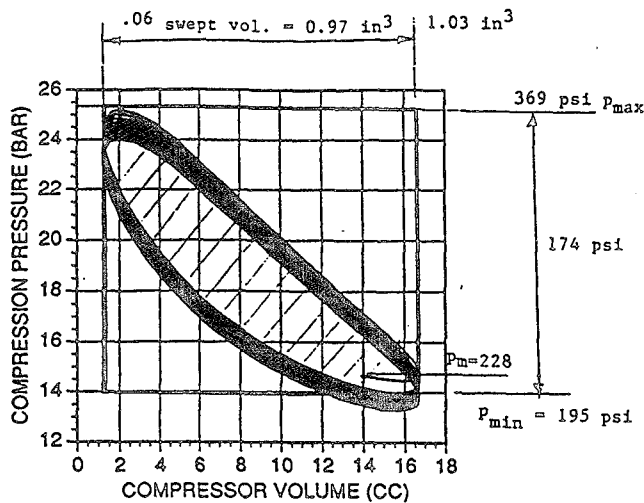
where f = operating frequency, p = pressure and v = volume. The integral, which represents the area of the PV diagram, can be estimated from specified pressure drop $2p_o$ and swept volume Δv using:

$$\int p dV = b (2p_o \Delta V)$$

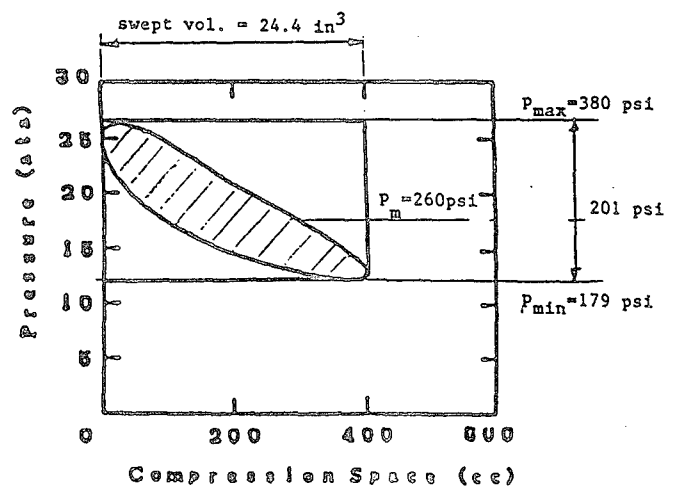
where b is a PV diagram factor. Typical values of this factor are determined from two typical PV diagrams shown in Figure 8. These diagrams are for: (a) for a 5W/65K cryocooler and (b) a 45W/80K cryocooler respectively. From these we found that b varies from 33% to 55% [7-8]. We can use these values as empirical range to estimate swept volume needed. For example, for the phase II compressor, $p_o = 50$ psi, $f = 40$ Hz, $P_{PV} = 20$ W and $b = 0.33$ yields $V_s = 0.14$ in³, which is close to 0.12 in³ swept volume specified.

Table 1. PV diagram factor b for two Typical Cryocoolers

Parameter	Name	5W/65K Cryocooler	45W/80K Cryocooler
p_m	mean pressure	228 psi a	260 psi g
p_{max}	maximum pressure	369 psi	380psi g
p_{min}	minimum pressure	195 psi	179 psi g
Δp	pressure drop	174 psi	201
V_{max}	maximum volume	1.03 in ³	24.4 in ³
V_{min}	clearance volume	0.06 in ³	0 in ³
ΔV	swept volume	0.97 in ³	24.4 in ³
f	frequency	26.7 cps	3.83 cps
$\int p dv$	area of PV loop	55.9 lb in	2737 lb in
$\Delta p \Delta v$	area of pv rect.	168 lb in	5672 lb in
b	pv factor	33%	55.8%



P-V diagram of a 5 W/65 K cryocooler :



P-V diagram for a 45W/80 K cryocooler

Figure 8. PV Diagrams of Two Typical Stirling Cycle Cryocoolers

3.3 Efficiency

A large portion of the power inputted is used to produce the output PV power. The efficiency η is defined as the ratio of the output PV power to the input power. The power inputted into the compressor can be computed from

$$P_{inp} = \frac{P_{PV}}{\eta}$$

For example, a compressor with $P_{PV} = 20$ W and $\eta = 0.7$ yields $P_{inp} = 29$ watts. The difference between input power and output power (i.e., 9 watts) constitutes a loss. This loss obviously should be minimized. These power losses are broadly divided into the I^2R losses in the drive coils, losses due to leakage of flux, core losses and hysteresis losses. Approaches to minimizing these power losses will be investigated in Phase II.

3.4 Pressure Wave

The pressure wave is specified usually by the mean pressure p_m and the pressure ratio r . It is also expressed in terms of other characteristic parameters [Marquardt 1993] using following formula:

$$\begin{aligned} p_o &= \frac{r-1}{r+1} p_m \\ p_{max} &= p_m + p_o \\ p_{min} &= p_m - p_o \\ r &= \frac{p_{max}}{p_{min}} \end{aligned}$$

where

r	=	pressure ratio
p_o	=	pressure wave amplitude
p_m	=	mean charge pressure
p_{max}	=	maximum pressure

p_{\min} = minimum pressure

For the model compressor, $p_m = 25$ psia and $r = 1.5$ yields

$$p_o = 5 \text{ psi}$$

$$p_{\max} = 30 \text{ psi}$$

$$p_{\min} = 20 \text{ psi}$$

4. DIAPHRAGM

The key to successful design of a diaphragm is to insure that the largest stress concentration is smaller than the smallest allowable fatigue stress. The diaphragm in Phase I was limited to a uniform flat design of constant thickness. Good insight into the effect of diaphragm's material and geometric parameters on the performance of the compressor is afforded by this simple geometry. This simplification allowed us to develop stress minimization schemes within the Phase I funding. The use of complex shaped variable thickness diaphragms could yield further reductions in stresses and improve the life, but this will be accomplished in Phase II of the project.

4.1 Design Requirements

The following compressor design requirements will impact the design of a diaphragm:

p_m = mean pressure	= 25 psia
r = Pressure ratio	= 1.5
max/min./amp pressure	= 30/20/5 psi
f = Frequency, cps	= 25 Hz
s = Stroke, mm	= 0.016 in. (0.4 mm)
V = swept volume	= 0.06 in ³ (1 cc)

In addition, a dominant requirement is that the diaphragm should not fail while generating the pressure wave. An ideal diaphragm should therefore :

- o develop least cyclic stresses
- o use minimum attraction force to generate largest pressure wave
- o be stiffer than the negative stiffness of electromagnets
- o be compatible with the working fluid of the cryocooler

For the prototype compressor, we size the diaphragm to meet following requirements:

- o develop a maximum stress of $\pm 10,000$ psi in the diaphragm
- o use least attraction force to generate a pressure wave of ± 5 psi
- o be stiffer than the negative stiffness of electromagnets
- o be compatible with gaseous helium

These requirements influence the stresses developed in the diaphragm and swept volumes produced. The design of diaphragm involves determining:

D = diameter of the diaphragm, in

t = thickness of the diaphragm, in.

E = Young's modulus of diaphragm material, psi

σ_{\max} = Maximum fatigue stress of diaphragm material, psi

In the following we assume that the diameter is given a priori as $D = 3.9$ in. The problem then reduces to finding t and E that can generate the specified ± 5 psi pressure wave without fatigue failure.

4.2 Load Analysis

The diaphragm's performance is determined by the type, magnitudes and phases of loads and their area of application. These loads are of two types - attraction loads and gas loads, and originate from the compression-chamber and back-chamber. The gas pressure is always compressive and acts over the entire diaphragm area while the attraction pressures are always tensile and act only over the pole area. In reality these loads vary with the displacement of the diaphragm. Hence they have a spring characteristic (force varies with displacement) instead of being constant (force is independent of displacement). We analyze this displacement dependency herein.

We broadly classify these loads as DC (or static) loads and AC (or dynamic) loads. The DC loads are constant, and do not change sign. They are considered positive if the diaphragm deflects out of the compression-chamber. The AC loads are variable and change sign; they are characterized by an amplitude and frequency. These are defined by the following notation:

Attraction Loads:

$-A_{dc}^c - A_{ac}^c \sin \omega t =$ Attraction electromagnet in compression-chamber

$+A_{dc}^b - A_{ac}^b \sin \omega t =$ Attraction electromagnet in back chamber

Gas Loads:

$G_{dc}^c + G_{ac}^c \sin (\omega t - \phi) =$ Gas load in compression-chamber

$-G_{dc}^b + G_{ac}^b \sin (\omega t - \phi) =$ Gas load in back chamber

where the symbol A denotes attraction load, G denotes gas load, c denotes compression chamber and b denotes back chamber.

4.2.1 DC Load

The DC load on the diaphragm is therefore given by:

$$P_{dc} = -A_{dc}^c + A_{dc}^b + G_{dc}^c - G_{dc}^b$$

The attraction and gas loads are estimated from analysis developed below. Note that, because these loads are distributed over different areas, the diaphragm may deflect even if the attraction pressure numerically equals gas pressure. In Phase I we use the double-acting electromagnet approach wherein the DC loads from the back chamber cancel those from compression chamber. This is accomplished by gas pressure equalization and bias current equalization. In Phase II we will examine the merits of single acting versus double acting diaphragm approach.

4.2.2 AC Load

The AC forces from the compression and back chamber add to each other. The ac load is

$$P_{ac} = -[A_{ac}^c \sin \omega t + A_{ac}^b \sin \omega t - (G_{ac}^c \sin (\omega t - \phi) + G_{ac}^b \sin (\omega t - \phi))]]$$

The AC attraction load should be sized to overcome not only the usable pressure wave in the compression-chamber but also that in the back chamber. The design constraint is that the smallest AC attraction pull must be used to get the largest diaphragm deflection while minimizing power consumption and stresses in the diaphragm.

(a) Attraction Load Analysis

The mechanism by which an electromagnet generates the attraction pull is shown in Figure 9. The attraction magnet consists of a coil of NI ampere turns wound around the central core of the electromagnet. The coil generated flux has a tendency to close the loop around itself using the shortest path that offers smallest resistance. The flux emanates from the coil passes through central pole into the air gap and thence into the diaphragm. It then flows radially outward in the diaphragm up to the fixed edge and thence completes the flux circuit through the clamped portion. The core and the coil transform the electrical energy into the magnetic energy. The magnetic energy is concentrated in the air gap of the central pole gap area. In this gap the magnetic energy is transformed again into mechanical energy. Because the diaphragm takes a cup-shape after deflection, this gap varies with radial position. But for our first order analysis, we assume it to be uniform. Analysis of a simple magnetic circuit - ignoring the leakage flux - shows that the flux in this gap is given by

$$\phi = \frac{\mu_o A_p NI}{g - x}$$

where

ϕ = gap in the flux circuit

A_p = area of the central pole

$NI(t)$ = ampere turns

g = mean gap between the diaphragm and the central pole

$x(t)$ = instantaneous deflection of diaphragm, positive if into compression-chamber

The diaphragm is sized to carry the flux produced by the two attraction magnets. Hence

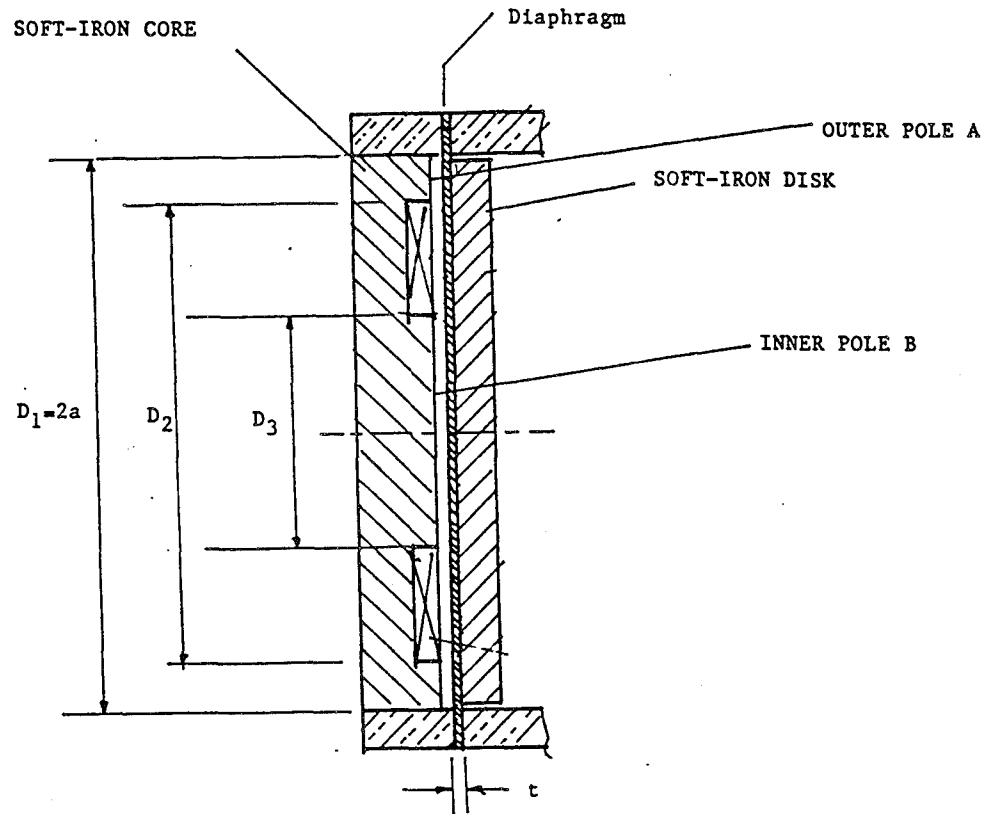


Figure 9. Method of Generation of Attraction Forces.

the gap flux density and diaphragm flux densities are given by

$$B_g = \frac{\Phi}{A_p} = \frac{\mu_o NI}{g - x}$$

$$B_d A_d = 2B_g A_g \quad \text{i.e.,} \quad B_d = \frac{2A_p}{A_d} \frac{\mu_o NI}{g - x}$$

$$B_d < B_{sat}$$

where

A_d = outer peripheral area of the diaphragm

B_d = flux density in the diaphragm

The attraction force is governed by

$$A(t) = \frac{B_g^2}{2\mu_0} A_p$$

where $B_{sat} = \text{gap flux density } (\phi/A_p)$. We suppose that the current contains both DC and AC components, $I = I_{dc} + I_{ac} \sin \omega t$, so that attraction force can be written as

$$A(t) = \frac{\mu_0 A_p}{2} \left[\frac{NI_{dc}}{g} \right]^2 \left[\frac{1 + I_{ac}/I_{dc} \sin \omega t}{1 - x/g} \right]^2$$

When AC currents are small relative to the DC currents and when diaphragm displacement is small relative to gap, we can rewrite the attraction force in terms of DC and AC components as

$$A(t) = A_{dc} + A_{ac} \sin \omega t \quad \text{where}$$

$$A_{dc} = \frac{\mu_0 A_p}{2} \left[\frac{NI_{dc}}{g} \right]^2$$

denotes the DC attraction force. Note that this DC force increases with the square of the ratio DC ampereturns/mean gap and varies directly with the pole area. It represents an upper bound to the AC component of attraction force which itself is given by

$$A_{ac} = k_i I_{ac} + k_x x \quad \text{where}$$

$$k_i = \frac{2A_{dc}}{I_{dc}}$$

$$k_x = \frac{2A_{dc}}{g}$$

The first equation above indicates that the AC attraction force depends not only on the AC currents but also on the displacement. The first term, called the current component, is created by the applied currents and hence requires external power. Its strength depends on the current stiffness k_i and strength of AC currents.

The second term, called the deflection component, is caused by the negative stiffness k_x (i.e., gradient of attraction force with displacement). This force is characteristic of the attraction electromagnet and does not require external energy. As the diaphragm moves closer to the

central pole, the gap reduces and hence the diaphragm experiences greater attraction force. This attraction gradient force aids the process of generation of pressure wave without consuming electrical power. This peculiar property of attraction electromagnets thus reduces the electrical power required to generate a specified pressure wave. As a result, the efficiency of electromagnetic compressors can be higher than that of piston-type compressors. A simple Fortran program was written to compute the attraction load using this analysis.

(b) Gas Spring/load analysis

Initially the active volume of compressor and the displacer is filled with He at a mean pressure P_m . The net volume of compressor and displacer is denoted by V . Let the mean pressure in the back chamber be $p'_m = p_m$ and its net volume is V . A displacement x of the diaphragm into the compression chamber translates into a pressure wave as described below.

The instantaneous displacement x increases the pressure in the compression space from p_m to $p(x)$ and reduces its volume from V to $V(x)$. The volume of the conical bulge shape of the deflection curve is approximated by $Ax/3$, (where A = area of the diaphragm) so that the instantaneous volume reduces to

$$V(x) = AL - Ax/3 = AL(1 - x/3L)$$

The adiabatic law $p_m V_m^\gamma = p(x) V(x)^\gamma$ yields the following instantaneous pressure $p(x)$

$$p(x) = p_m (1 - x/3L)^{-\gamma}$$

The pressure wave $p_o(x)$ in the compression chamber is the difference between this instantaneous pressure and the mean pressure, and is given by

$$p_o(x) = p(x) - p_m = p_m [(1 - x/3L)^{-\gamma} - 1]$$

Figure 10 is plot of normalized gas spring force $p_o(x)/p_m$ assuming isothermal conditions ($\gamma = 1$). From this figure, it is clear that the amplitude of pressure wave depends on the displacement x

(relative to the length of the compression chamber). For the prototype, $p_o = 10$ psi, $p_m = 30$ psi yields $p_o/p_m = 0.33$. For this data, this figure shows that x/L should be 0.75 to achieve this value. Since $L = 0.013$, the diaphragm should vibrate by $x = \pm 0.010$ in. to achieve the specified dynamic pressure of ± 10 psi.

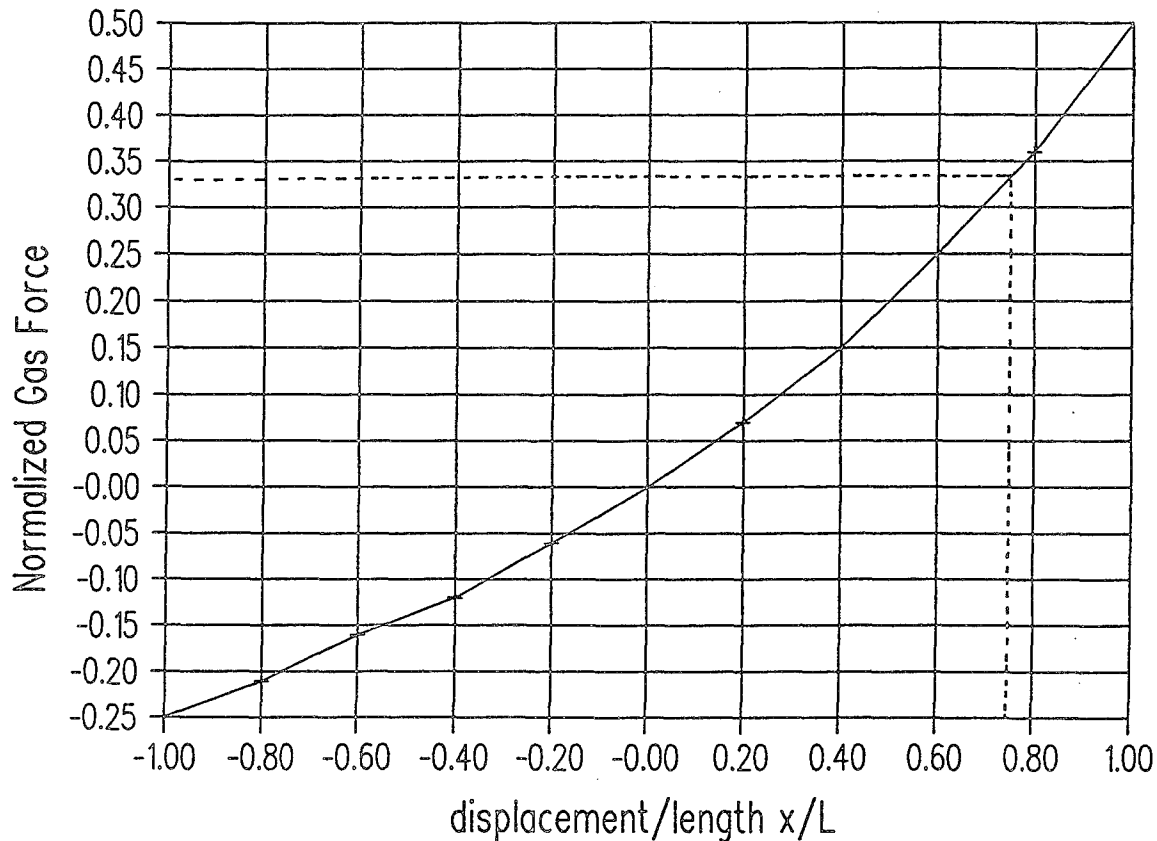


Figure 10. Gas Spring Force (in Compression Chamber) For a Given Diaphragm Displacement.

Consider the Back Chamber. The displacement x reduces the pressure from p_m to $p'(x)$ and increases the volume from V_o' to $V'(x)$. Adiabatic law yields the instantaneous back pressure $p'(x)$ and associated back pressure wave $p'_o(x)$

$$p'(x) = p_m (1 - x/3L)^{-\gamma}$$

$$p_o(x) = p'(x) - p_m = p_m [1 - x/3L)^{-\gamma} - 1]$$

This back spring force is obviously a mirror image of the gas spring force. The gas spring force is determined from gas pressures in the compression space and back chamber. This force will always oppose the displacement and is directed towards the position of static equilibrium $x = 0$. It is given by

$$g(x) = [p(x) - p'(x)] A \\ = \frac{(6x/L)}{9 - (x/L)^2} p_m A$$

Figure 11 shows this normalized net gas force $g(x)/p_m A$ as a function of displacement under isothermal conditions. From this figure, it is clear that the net spring rate of the gas pressure is nearly linear. The gas force can thus be approximated by a gas spring

$$g(x) = \frac{3p_m A}{4L} x = k_g x$$

where

k_g = gas spring rate, lb/in.

$p_m = 10$ psi, $A = 11.95$ in², $L = 0.013$ in. and $\gamma = 1$ leads to gas stiffness of $k_g = 6900$ lb/in.

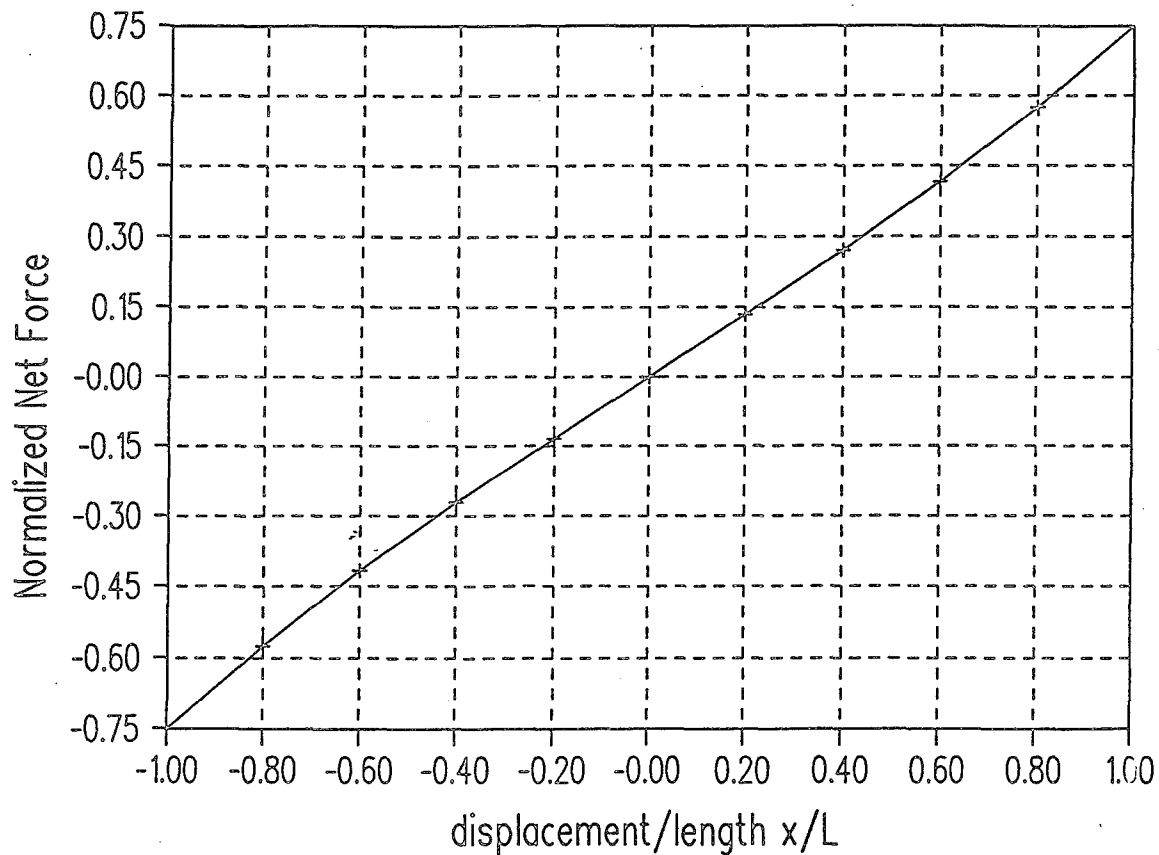


Figure 11. Normalized Net Gas Force vs. Displacement.

4.3 Deflection Analysis

Since the loads are axi-symmetric, the deflection varies with the radial position only. The deflection of the diaphragm obviously depends on the attraction and gas pressures. They can be computed from formulas available from several sources [10-13]. These formulas are based on thin plate theory, i.e., deflections are assumed to be smaller than the thickness. In our case the deflection can be larger than the thickness, so the non-linearity should be taken into account. The small deflection formulas however have the added advantage that superposition principle can be used to describe the behavior under a variety of diaphragm loading arrangements. A simple Fortran program was written to obtain the deflection contours, stresses and swept volume. This program was validated by hand-calculations for several cases of diaphragm dimensions and loadings.

While testing the Phase I compressor model, we discovered a phenomenon we called "hump effect". This phenomenon is characterized by the inner region of diaphragm being pulled inwards by the attraction load and the peripheral regions pushed outward by the gas loads. The attraction load -acting through pole area - pulls the diaphragm into the compression chamber. On the other hand, the compressive gas load - acting over a larger diaphragm area - pushes the diaphragm out of the compression-chamber. The deflection contour is the resultant of these two actions. Because attraction pressure acts through the pole area and the gas pressure acts over the larger diaphragm area, it is possible that, for certain combinations of attraction and gas pressures, the central portion of diaphragm (facing the pole) will be deflected inwards while the remaining portion might project out of the compression chamber as a "hump". This "hump" reduces the swept volume. Obviously the attraction pressure must be sized to avoid this "hump" phenomenon.

In order to overcome the hump phenomenon, it is necessary to accurately estimate the shape of the deflection curve under widely varying loads. The diaphragm deflection can be broken into DC deflection - due to DC loads and AC deflection - due to AC loads. It is assumed that the DC loads are zero, so the DC deflection is zero. Hence we focus on AC deflections due to AC load only. These loads are given by equation (5). The superposition principle is used to calculate the net deflection under these variety of loads. In general, the central deflection is estimated from

$$k x = f$$

where

k = stiffness of diaphragm under load f

x = deflection of diaphragm

f = AC load on the diaphragm

The stiffness of diaphragm can be estimated from known formulas such as those given in Roark.

Let us assume that the compression and back chambers are identical. The central deflection due to attraction loads, which contain the AC current component and deflection component, is computed from

$$\begin{aligned}
k_a x &= A_{ac}^c + A_{ac}^b \\
&= 2k_f I_{ac} + 2k_x x \quad \text{i.e.,} \\
(k_a - 2k_x)x &= 2k_f I_{ac}
\end{aligned}$$

where

k_a = stiffness of diaphragm under attraction load

From this it is clear that the net stiffness is the diaphragm stiffness minus twice the negative stiffness. Since net stiffness is softer than the diaphragm, smaller current will be required by the electromagnet.

The central deflection due to the gas loads are similarly calculated using gas springs. Note that the effect of gas springs is to increase the net stiffness whereas the effect of attraction stiffness is to reduce it. Accurate estimation of stiffness of these springs is therefore vital to determining the central deflection of the diaphragm.

4.4 Stress Analysis

The dynamic or AC stresses in the diaphragm are of significant interest as they strongly influence the fatigue life of the machine. The phase difference between the pressure wave and deflection also influences the stress amplitudes. In Phase I however, to simplify the analysis, we assume that the attraction pressures are 180 degrees out of phase with the gas pressure wave. During one complete cycle, the diaphragm will fully deflect into the back cavity plate, reverse itself and fully deflect into the compression cavity plate. The stresses in the diaphragm are the membrane radial stress, membrane tangential stress and the bending tangential stress. These stresses are then combined algebraically to yield maximum stress which governs the life of the diaphragm. The combined stress is maximum at the inflection point and at the center of the cavity. The inflection point is the point where the two radii are tangent to each other. For small deflections of thin plate loaded by pressure q spread from radius $r = r_0$ to $r = a$, the radial and tangential stresses can be computed from the formulas

$$\sigma_r = \frac{6M_r}{t^2} ; \quad \sigma_t = \frac{6M_t}{t^2} \quad \text{where}$$

$$M_r = M_c + T_M$$

$$M_t = \frac{(1-\nu^2)D}{r} \theta + \nu M_r$$

where the constants are given by

$$M_c = (1+\nu)a^2 q L_{14}$$

$$\theta = \frac{r M_c}{D(1+\nu)} + T_\theta$$

$$T_M = -qr^2 G_{17}$$

$$T_\theta = -\frac{qr^3}{D} G_{14}$$

$$L_{14} = \frac{1}{16} [1 - b^4 - 4b^2 \ln(1/b)]$$

$$G_{14} = \frac{1}{16} [1 - c^4 - 4c^2 \ln(1/c)] <r-r_o>^0$$

$$G_{17} = \frac{1}{4} [1 - \frac{1-\nu}{4} [1 - c^4] - c^2 [1 + (1+\nu) \ln(1/c)] <r-r_o>^0$$

$$b = \frac{r_o}{a}$$

$$c = \frac{r_o}{r}$$

The deflections are usually larger than half the thickness of the diaphragm. In such cases, the middle surface becomes appreciably strained and the stress in it, called the membrane stress, cannot be ignored. This stress enables the diaphragm to carry a part of the load in direct tension.

Under these conditions, the maximum stress can be estimated from (see Roark, p. 433)

$$\sigma = \frac{(4.267 tx + 0.476 x^2)}{a^2} E$$

where

σ = maximum stress in the diaphragm

t = thickness of diaphragm

x = maximum deflection of the diaphragm

E = Young's Modulus

4.5 Diaphragm material

The diaphragm material must be carefully selected to meet the long life requirement. The most popular materials are Ti-6Al-4V and stainless steels. Major considerations in selecting the diaphragm material are:

- o it must operate without failure over 10^{10} fatigue cycles
- o it should be capable of developing large deflections without failure
- o it must not react with Helium
- o its outgassing must be very low
- o it should be available in the thin sheets 0.010 - 0.080 in.
- o it must be light weight (high strength to wt. ratio).

In order to have long life, ideally, a diaphragm should have

- o high yield strength to yield the long life requirement
- o low Young's Modulus to meet the large swept volume/pressure wave requirement

A high yield strength ensures that the diaphragm will carry large stresses without failure. A low Young's modulus on the other hand makes the diaphragm flexible enough to create a large swept volume. A high yield strength/Young's modulus will therefore signify longer life while delivering larger swept volume. The ratio of yield strength to Young's modulus is called the life factor σ_E .

$$\sigma_E = \frac{\text{Yield Strength } \sigma_{yld}}{\text{Young 's Modulus } E}$$

The central deflection is proportional to the ratio of maximum stress and Young's modulus.

Since higher deflection obviously means higher swept volume and hence higher pressure wave, to maximize the pressure wave, high life factor is desirable. Thus, the most appropriate material for the diaphragm is one which has the largest life factor.

Recognizing the importance of the life factor, we have collected data on this value for various materials. These materials may be broadly classified into metallic and non-metallic. We note that nonmetallic materials can be as strong as metallic materials. But we eliminated them for space cryocooler application as they have significantly higher outgassing than metallic materials. Table 1 below indicates the life factor of typical metallic and non metallic materials.

Table 1. Long Life Factor σ_E for Membrane Materials (at 300 K)

N o.	Material	Density lb/in ³	Yield Strength σ_{yt} ksi	Endur- ance Limit σ_{end} ksi	Young's Modulus E 10 ⁶ psi	Long life Factor $\sigma_E = \sigma_{yt}/E$	Ref.
1.	Ti-6Al-4V Annealed	0.160	120 ⁷	80 ^a	14 - 19	8.6	5 - 6
2	Chromium steel 7C27M02	0.3	210	210/2 = 100	30	7	7
2.	Maraging Steel 18Ni(300)	0.3	280	280/2 = 140 ^b	27	10.4	
3.	Be-Cu 172, 1-2 Hard	0.3		80 ^a	18	4.4	6
4.	Stainless Steel 321 Annealed	0.29		42 ^a	28	1.5	6
5.	Aluminum 6061- T6	0.097		30 ^a 14 ^c	10		
6.	Polyamid Nylon 6 Comturf 613	.048	272	135 ^b	1.0	272	
7.	Polyster Glass Fibre Reinf. Hyside 11 YRr.	0.068	240				
8.	Polyster Woven Glass Cloth		80	40 ^b	2.5	32	

- a) At 77K (see Ref. 11)
- b) Considered as half of flexural yield strength
- c) see ref 11
- 7) Guaranteed min. per catalog R President Titanium, Hanson, MA 02341.

From this table it is clear that Titanium alloy Ti-6Al-4V and maraging steel are ideal metallic materials. The beryllium copper has a lower life factor than the two and hence is not preferred. Since we need a magnetic material for the diaphragm (in order to attract the electromagnet), we believe that maraging steel is an ideal candidate. However, this steel is not available in sheet form so we prefer the next best, viz. chromium stainless steels as possible candidate.

5.2.6 Permissible Working Stress

A membrane vibrating at 60 Hz for 10 years undergoes 2×10^{10} cycles of reversal of stress. Fatigue data at these large number of cycles is not readily available. Hence we rely on the

$$N = \frac{\text{Yield Strength } \sigma_{yld}}{\text{Max. Working Stress } \sigma_{max}}$$

"Fatigue Safety Margin N" concept. It is defined above. The yield strength is taken at 0.2 % amplitude. The maximum working stress is the amplitude of cyclic stress that will ensure fail-safe operation up to 2×10^{10} cycles. As rule of thumb, we take $N = 10$ or greater to ensure life of ten years as per the rationale given below.

Wong et al [3] indicates that for a high quality stainless steel, spring material, the peak stress should be limited to one-half of the endurance limit, or 415 MPa (60,000 psi) in order to achieve the 10 year life requirement. Since endurance limit is usually one-half of yield strength, the Fatigue Safety Margin according to him is $N = 4$.

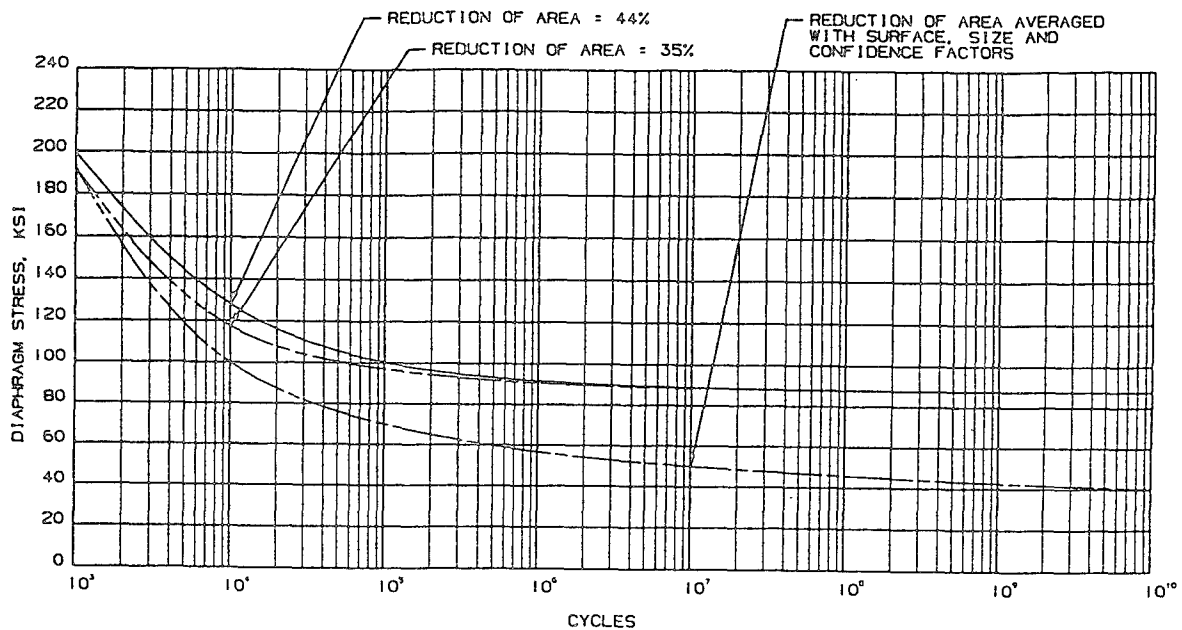
In contrast, Stacy [11] indicates that the membrane stresses should be less than 90 MPa

(13,000 psi) to achieve long life. In fact, Stacy says that 100 MPa peak stress limit falls well below 99.999% fatigue probability at 10^{10} cycles of recurring stress. The yield stress is 120 ksi for the Ti-6Al-4V material he used. The Fatigue Safety Margin is $N = 9$.

Thus, there is a significant difference in the Fatigue Safety Margins specified by the two experts. Therefore, as a matter of abundant precaution, we choose $N = 10$. This yields a maximum working stress of 10,000 psi for a Ti-6 Al-4V material. Our decision to limit stresses to 10000 psi will exceed both above safety margins and hence will have long life.

A classic fatigue curve, such as that shown in Figure 12 shows that as the stress level is increased, the number of cycles to failure decreases. Conversely, as the stress level is decreased, the number of cycles to failure increases. Typically, a stress level of 100 ksi results in a life of 100 to 1000; a stress level of 75 ksi will yield a life of 10^4 to 10^5 cycles. Finally by dropping the stress level to 75 ksi, the life goes up to 10^8 . Reducing it further to about 20 ksi will increase the life further to 10^{10} .

Consider a strain hardened, cold rolled 301 SS material whose properties are far in excess of annealed material. This material however is non-magnetic and hence could not be selected for our compressor. The yield strength of this material is 180,000 psi. A fatigue life drawing such as figure indicates that a design stress below 40 ksi can reach life of 10^{10} cycles.



THESE CURVES ARE BASED ON DIAPHRAGM MATERIAL
FOLLOWING MECHANICAL PROPERTIES:

ULTIMATE TENSILE STRENGTH - 190,000 PSI, MIN.
 YIELD STRENGTH - 180,000 PSI, MIN.
 ELONGATION - 15% MIN.
 REDUCTION OF AREA - 35 TO 44%
 HARDNESS - 38 TO 45 RC

Figure 12. Fatigue Curves of a typical high strength material

5.2.7 Fatigue Analysis

Since the membrane fails by flexure, the flexural yield strength can be taken as a rough measure of the fatigue strength. However, this data is not readily available for many materials, so yield strength is taken as a primary measure of fatigue strength.

Since diaphragm stresses are cyclic, the cyclic stress must be addressed during the design stage itself. The fatigue data can broadly be classified into low cycle data, which is determined by strain cycling to a level that is beyond the yield strength. A common example is tensile test to determine the yield strength elongation etc. A high cycle fatigue data is accumulated while the material is being stressed in the elastic strain region.

In addition to the stress, factors that influence the fatigue life are:

o *Surface finish* - The surface finish of the diaphragm must be highly polished and smooth to be free of nicks, scratches and metal inclusions in order to attain high cycles. Surface scratches and nicks produce stress concentrations of varying magnitude ranging from 1 to 3 and the stress level will increase rapidly.

o *Tensile Strength* - Higher tensile strength usually yields higher fatigue life. However, when tensile strength is increased, the material becomes very notch sensitive, and a point is reached when additional strength compromises toughness.

o *Thickness* - The stresses are inversely proportional to the thickness to produce a given pressure wave. When the thickness is less than 0.010 in., the material is difficult to handle and cannot stand negative stiffness. Typical diaphragms therefore range from 0.015 to 0.020 in thickness. Other things being equal, a thinner material will fail sooner than thicker material due to crack propagation.

o *Cavity shape* - The shape of the cavity exerts the greatest influence on the stress level. The cavity must be precisely machined, preferably using a numerically controlled lathe with the cavity automatically generated by a program. Once the cavity is cut, it must be inspected using a cavity plotter to verify the contour within 0.001 in. Maintenance in the field can also be an important factor. Excessive polishing or lapping the head could unfavorably change the stress levels.

o *Torque* - The head bolts must be torqued in a cross pattern, incremental and to specific levels. If the edges of the diaphragm are not uniformly clamped and restrained, the stresses in it change significantly.

o *Cleanliness* - Dirt in any form will change the cavity shape and cause stress concentrations. The smallest of the particles that enter into the cavity will usually work their way to the outer edge and build up on the surface adjacent to the clamped seal area. Larger particles will cause stress concentrations and can change stresses by a factor of 1.2 to 3.

o *Fretting Corrosion* - This fretting occurs when there is low frequency relative motion between two elements under load. Metal is removed from one element and this sets up stress concentration, usually in the diaphragm. To reduce the fretting, the contact surfaces must be

relieved. In addition, high temperatures will affect the diaphragm stresses significantly.

301 Steel. A strain hardened, cold rolled 301 SS material has properties that are far better than that of annealed material. The yield strength of this material is 180,000 psi. A fatigue life drawing such as figure 12 indicates that a design stress below 40 ksi can reach life of 10^{10} cycles. This material is non-magnetic and hence could not be selected for our compressor.

Sandvik 7C27M02 steel. This steel sheet has a tensile strength of 261,000 psi. It has a fatigue limit of 125,000 psi. Limiting the stress to 10,000 psi will therefore greatly increase the confidence that it will work without failure.

4.6 Dynamic Model of the Diaphragm

The diaphragm can be modeled in a number of ways. In the following f denotes the net attraction force and g denotes the net gas force. The first model is the static model $kx = f_0 - g_0$, [used by Creare, Stacy and Shimko 2] which ignores the dynamic effects and assumes that the diaphragm deflects statically. The next refinement is the pressure wave model $m \ddot{x} + c \dot{x} + kx = f(t) - g(t)$ which assumes that attraction and gas pressure do not change with displacement. This model was used by Marquardt, Radebaugh, Kittel [9]. A further refinement is the gas spring model $m \ddot{x} + c \dot{x} + kx + g(x) = f(x)$ which recognizes that the attraction and gas forces behave as non-linear spring. This model recognizes that gas pressures change with the displacement. This model was used by Sussholz [10] for pressure sensors and Jonge [11] and Boyle et al [12] for piston-driven compressors. We will investigate this model in Phase II.

Note that in Phase I we deal with an unloaded compressor. The model is not connected to a displacer. As such the pressure wave that is generated will be confined to the compression chamber. This pressure wave is not transmitted into a displacer. In this sense the Phase I compressor does not realistically depict its performance. In the real world, the compressor is always connected to a displacer using a small tube. The volume of the displacer chamber adds to that of the compression chamber and this effects the strength of the pressure wave. In Phase II we will develop the more realistic model of the loaded compressor which includes the effect of volume of displacer.

We make following assumptions in developing the model: (1) The pressure within the compression chamber follows the law of adiabatic compression [13], $PV^\gamma = \text{constant}$, $\gamma = 1.4$ (2) The dissipative forces such as heat loss, friction and leakage are small, and can be modeled by a linear viscous damper. (3) The internal pressures are uniform throughout, and diffraction effects at the mouth of the outlet are negligible. (4) The continuous diaphragm can be modeled by an equivalent discrete mass-spring system.

From the free body diagram shown in Figure 13, the displacement x is governed by

$$m \ddot{x} + c \dot{x} + k_d x = f - g(x)$$

where

m = effective mass of the diaphragm, lb/g

c = effective damping coefficient of the system, lb-sec/in

k_d = effective stiffness of the diaphragm, lb/in

$x(t) = x_c \sin(\omega t - \phi)$ = instantaneous displacement of diaphragm's center, in

$g[x(t)] = g_o[x] \sin(\omega t - \psi)$ = restoring gas force on the diaphragm

$f[x(t)] = f_o[x] \sin \omega t$ = applied attraction force on the diaphragm

Initially, there is no attraction force; compression and back chamber pressures are equal and opposite. So the diaphragm is in equilibrium at $x = 0$.

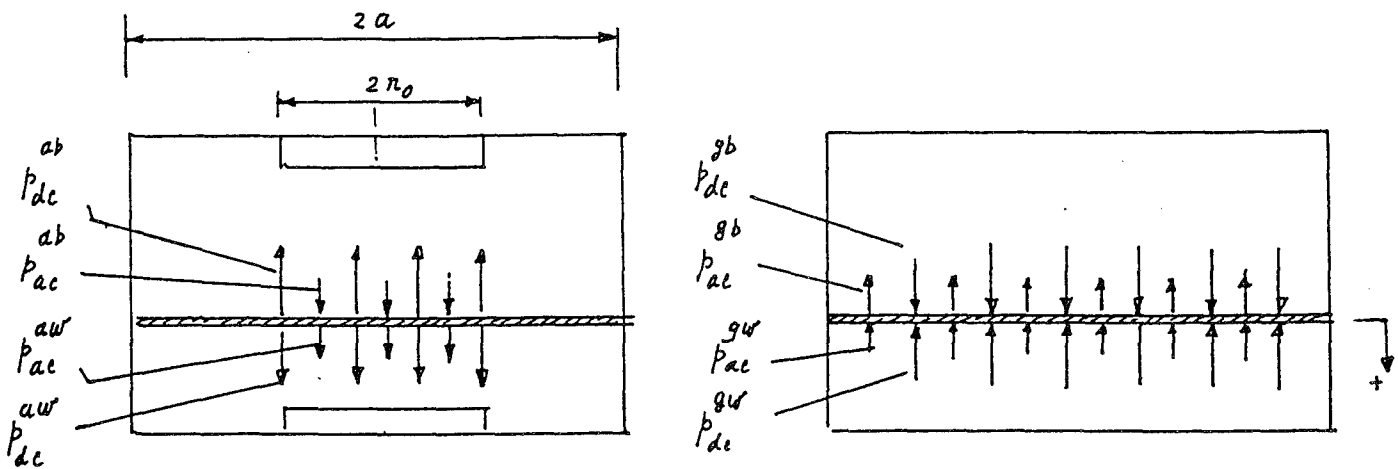


Figure 13. Free Body Diagram of the Diaphragm.

4.6.1 Estimation of Attraction Force

The attraction pressure p_a moves the diaphragm to the right, which increases the fluid pressure in the right captive chamber from p_m to $p_m + p_o \sin(\omega t - \psi)$. It also reduces pressure in the left chamber from p_m to $p_m - p_i \sin(\omega t - \psi)$. The dynamic pressures p_o and p_i push the diaphragm to the left. In other words, the attraction pressure is always opposed by the dynamic pressures it creates. Let x_c denote the central deflection of the diaphragm under the combined action of p_a , p_o and p_i . The swept volume V_s during peak-to-peak displacement is the twice conical volume contained by base diameter $2a$ and the central deflection x_c , and is given by

$$V_s = \frac{2}{3} \pi a^2 x_c$$

The dynamic pressure amplitude is related to this swept volume by:

$$\frac{P_o}{P_m} = \frac{V_s/2}{V_r}$$

Substituting (2) in (3) shows that the central deflection can be computed from specified pressure wave amplitude by

$$x_c = \frac{V_r}{\pi a^2/3} \frac{P_{dyn}}{P_o}$$

5. COMPRESSION CHAMBER

5.1 Design Requirements

The compression chamber provides a dirt-free space for creating a specified pressure wave. The volume between a vibrating diaphragm and the contour of cylinder defines this compression space. The design objective is to size this volume from the following data:

p_m	= mean charge pressure
r	= pressure ratio
α	= ratio of deflection volume and swept volume
ΔV	= swept volume
V_p	= payload volume
γ	= specific heat ratio

In addition, we assume that the diameter D of the compression chamber is specified a priori. The mean captive volume is the initial volume into which the working fluid is charged. It comprises of the pay load volume (displacer volume) and the compression chamber volume. The net volume . It is broken into a deflection volume and a dead volume. The deflection volume is the volume between the undeflected and deflection positions of the diaphragm. The dead volume is the balance of mean captive volume that is left after the diaphragm fully deflects. The volume parameters to be determined are hence:

V	= mean captive volume ($= V_p + V_w$)
V_w	= compression chamber volume ($= V_D + V_d$)
V_D	= deflection volume ($= \alpha \Delta V$)
V_d	= dead volume ($= V_w - V_D$)

The adiabatic gas law $PV^\gamma = \text{const.}$ will be used to size the compression chamber. This law defines the behavior of an ideal gas when its volume changes with no heat entering or leaving.

This condition is usually satisfied during the compression phase when pressure changes from P_m to P_{max} and volume changes from V to V_{min} . [The diaphragm movement gives rise to gas flow causing the pressure difference and the displacer position determines the amount of gas in compression and expansion spaces; these effects are ignored in our elementary model]

$$\frac{P_{max}}{P_m} = \frac{V_m^\gamma}{V_{min}^\gamma} = \frac{2r}{r+1} \quad (a)$$

Noting that minimum and mean captive volumes are given by:

$$\begin{aligned} V_m &= V_p + V_w \\ V_{min} &= V_p + V_w - \alpha \Delta V \end{aligned} \quad (b)$$

Using (b) in (a) yields following expression for compression chamber volume:

$$V_w = \frac{\alpha R}{R-1} \Delta V - V_p \quad \text{where } R = \left(\frac{2r}{r+1}\right)^{1/\gamma} \quad (1)$$

This compression chamber volume is used to compute the volume parameters using:

$$\begin{aligned} V_m &= V_p + V_w \\ V_D &= \alpha \Delta V \\ V_d &= V_w - V_D \end{aligned} \quad (2)$$

Axial Length of Compression Chamber

The axial length of a cylindrical compression chamber is computed from:

$$\frac{\pi}{4} D^2 L = V_w \quad \text{i.e., } L = \frac{4V_w}{\pi D^2}$$

where L = axial length of a noncontoured compression chamber.

If this L is found to be less than maximum central deflection, then a contoured compression chamber will be required. Using a cone approximation formula, the axial length of a contoured

compression chamber will be found from:

$$\frac{1}{3} \frac{\pi}{4} D^2 L = V_w \quad \text{i.e.,} \quad L = \frac{12 V_w}{\pi D^2}$$

5.2 Back chamber

The back chamber's primary function is to balance the diaphragm against the charge pressure. This charge pressure pushes the diaphragm outward and creates static stresses in it. There are two methods to counter this action of charge pressure:

(a) Sealed Back Chamber Approach. (Figure 14a). This approach uses two attraction electromagnets, one is the compression chamber and another is the back chamber (i.e., it requires electromagnets on both sides of the diaphragm). The back chamber is charged with gas at mean pressure and is sealed. The diaphragm thus remains at the neutral position under the action of two equal and opposite gas pressures as shown in this Figure. However, this approach has the disadvantages that it creates a pressure wave in the back chamber (that is not used in the cryocooler). This unused pressure wave opposes the displacement of the diaphragm. The attraction magnet should therefore overcome this unused pressure in addition to the useful pressure wave in the compression chamber. So this approach increases external force required without increasing the output compression. As such, this approach is not a preferred method.

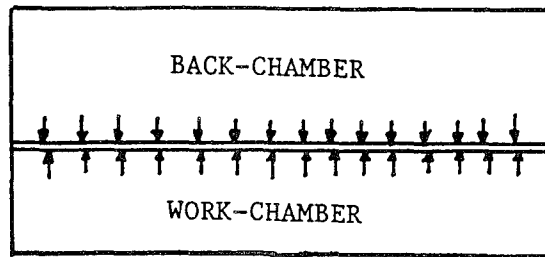
(b) Open Back Chamber Approach (Figure 14b). This uses a single electromagnet on the compression-chamber. It does not use any back chamber (i.e., one side of the diaphragm is left open to atmospheric pressure). It uses a permanent magnet bias to neutralize the DC stress produced by the charge pressure. This permanent magnet can be positioned in the cylindrical face of the compression chamber as shown. As a result the diaphragm initially deflects inwards into the TDC. The compression chamber is then charged with pressurized gas to bring it back to the mean position. The magnet is sized so that its attraction force balances the charge pressure and positions the diaphragm at its neutral position.

The advantage of this approach is that, unlike the sealed back chamber approach, it does not

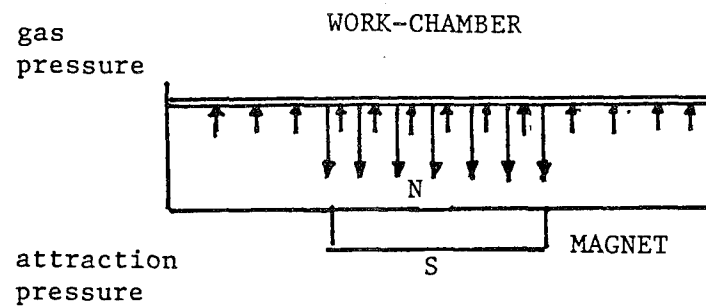
create an additional, but unused pressure wave in the back chamber. As a result, this approach requires less attraction force than that needed by the sealed back chamber approach. The use of a smaller attraction force obviously saves significant input power, and hence this approach is the preferred approach. This approach will be investigated in the Phase II of the project.

To qualify the advantage of the open back chamber approach we considered the problem of generating a 25 ± 8.33 psi pressure wave. We used a 3.9 in diameter 0.015 thick steel diaphragm to generate this pressure wave. The sealed back chamber approach produced an additional ± 8.33 psi pressure wave. Our computations showed that a ± 30 psi attraction pressure (at 1.0 pole diameter) will be required to overcome the net ± 16.67 psi pressure wave on the diaphragm if the sealed back chamber approach is used.

If the open back chamber approach is used, the attraction pressure needs to overcome ± 8.3 psi of pressure wave in the compression chamber only. As a result our analysis indicates that the attraction pressure can be reduced from ± 30 psi to ± 15 psi. As a result we save half the power needed to produce the desired pressure wave.



(a) Back-chamber approach



(b) PermanentMagnet Approach

Figure 14. Two Design Approaches to Back Chamber Design.

CONCLUSIONS

This report presented the investigations carried out by Precision Magnetic Bearing Systems under an SBIR project sponsored by Ballistic Missiles Defense Organization. The report addressed the issue of feasibility of a novel electromagnetic diaphragm compressor to drive cryocoolers. Two prototype compressor units were built to establish the feasibility. The first prototype used permanent magnets to bias the vibrating diaphragm while the second prototype used electromagnets. The diaphragm used in the first prototype was found to be too stiff and hence electromagnet was used in the second prototype together with a thinner diaphragm. Testing of the second prototype indicated that it is possible to develop pressure ratios of the order of 1.67 at frequencies of up to 60 Hz. Since cryocoolers require pressure ratios of about 2 at frequencies of about 40 Hz, it is concluded that it is feasible to develop an engineering model of the compressor to drive cryocoolers.

REFERENCES

- [1] Kroger, J., "Magnetic Actuator Concepts and Applications", NASA Conference Publication No. 3202, pp. 5-18, 1988.
- [2] Stacy, W.D., and Shimko, M.A., "An Ultrareliable Cryocooler for Satellite Sensor Cooling", Project Report under Contract No. DNA0001-87-C-0199, 1988.
- [3] Shimko, M.A., Stacy, W.D., McCormick, J. A., "Engineering Model Cryocooler Test Results", Proc. IECEC, 1992, Vol. 5, pp. 5.81-5.86
- [4] Stacy, D., McCormick, J., and Valenzulea, J., "Development and Demonstration of a Diaphragm Stirling 65 K standard spacecraft cryocooler," Proc. 7th International Cryocooler Conference, Nov 17-19, 1992, Santa Fe, pp. 40-49.
- [5] Stacy, W.D., " A 10 year life 65 K Stirling Cryocooler for Satellite Sensor Applications", Proc. 6th International Cryocooler Conference, Plymouth, MA, Oct. 1990.
- [6] Diaphragm Actuator for Stirling microrefrigerator, Sun Power, OH, Phase I SBIR, NASA 1991.
- [7] Yuan, S.W.K and Spradley, I.E., "Validation of the Stirling Engine Refrigerator Performance Model Against Philips/NASA Magnetic Bearing Refrigerator" Proc. 7th International Cryocooler Conf., Sante Fe, 1992, pp 280-289.
- [8] Ishizaki, Y and Ishizaki , E, "Experimental Performance of Modified Pulse Tube Refrigerator below 80 K down to 23 K" Proc. 7th International Cryocooler Conf., Sante Fe, 1992, pp. 140-146.
- [9] Marquardt, E., Radebaugh, R and Kittel, P "Design Equations and Scaling Laws for Linear Compressor with Flexure Springs", Proc. 7th Cryocooler Conf., Sante Fe, 1992, pp. 783-804.
- [10] Sussholz, B., "Forced and Free Motion of a Mass on an Air Spring", Journal of Applied Mechanics, June 1944, pp. A101-A107.

- [11] Jonge, A.K., " A Small Free-Piston Stirling Engine", IECEC Conference Paper No. 799245, 1979.

- [12] Boyle, R., Connors, F., et al "Non-real time, Feed Forward Vibration Control System Development and Test Results", Proc. 7th International Cryocooler Conference, Nov. 1002, Santa Fe, 1992, pp. 805-819.

- [13] Bradshaw, T.W., Orlowska, A.H., and Hieatt, J., "Computer modelling of Stirling Cycle Cryocoolers", Proc. 7th International Cryocooler Conference, Nov 1992, pp. 772-782.

- [12] Tward, E and Sarwinski, R., "A Closed Cycle Cascade Joule Thomson Refrigerator for Cooling Josephson Junction Devices", Proc. Third Cryocooler Conference, p . 220-1986.

DISTRIBUTION LIST

AUL/LSE Bldg 1405 - 600 Chennault Circle Maxwell AFB, AL 36112-6424	1 cy
DTIC/OCC Cameron Station Alexandria, VA 22304-6145	2 cys
AFSAA/SAI 1580 Air Force Pentagon Washington, DC 20330-1580	1 cy
PL/SUL Kirtland AFB, NM 87117-5776	2 cys
PL/HO Kirtland AFB, NM 87117-5776	1 cy
Official Record Copy	
PL/VTPT/Brian Whitney	2 cys
Dr. R. V. Wick PL/VT Kirtland, AFB, NM 87117-5776	1 cy